

NAVAL POSTGRADUATE SCHOOL

Monterey, California



DIELECTRIC LOADED FINNED
WAVEGUIDE STUDY

Jeffrey B. Knorr

March 1977

Approved for public release; distribution unlimited.

Prepared for: Naval Electronics Laboratory Center
Microwave Technology Branch - Code 2330
San Diego, CA

FEDDOCS
D 208.14/2:
NPS-62KO77031A

NAVAL POSTGRADUATE SCHOOL
Monterey, California

Rear Admiral Isham Linder
Superintendent

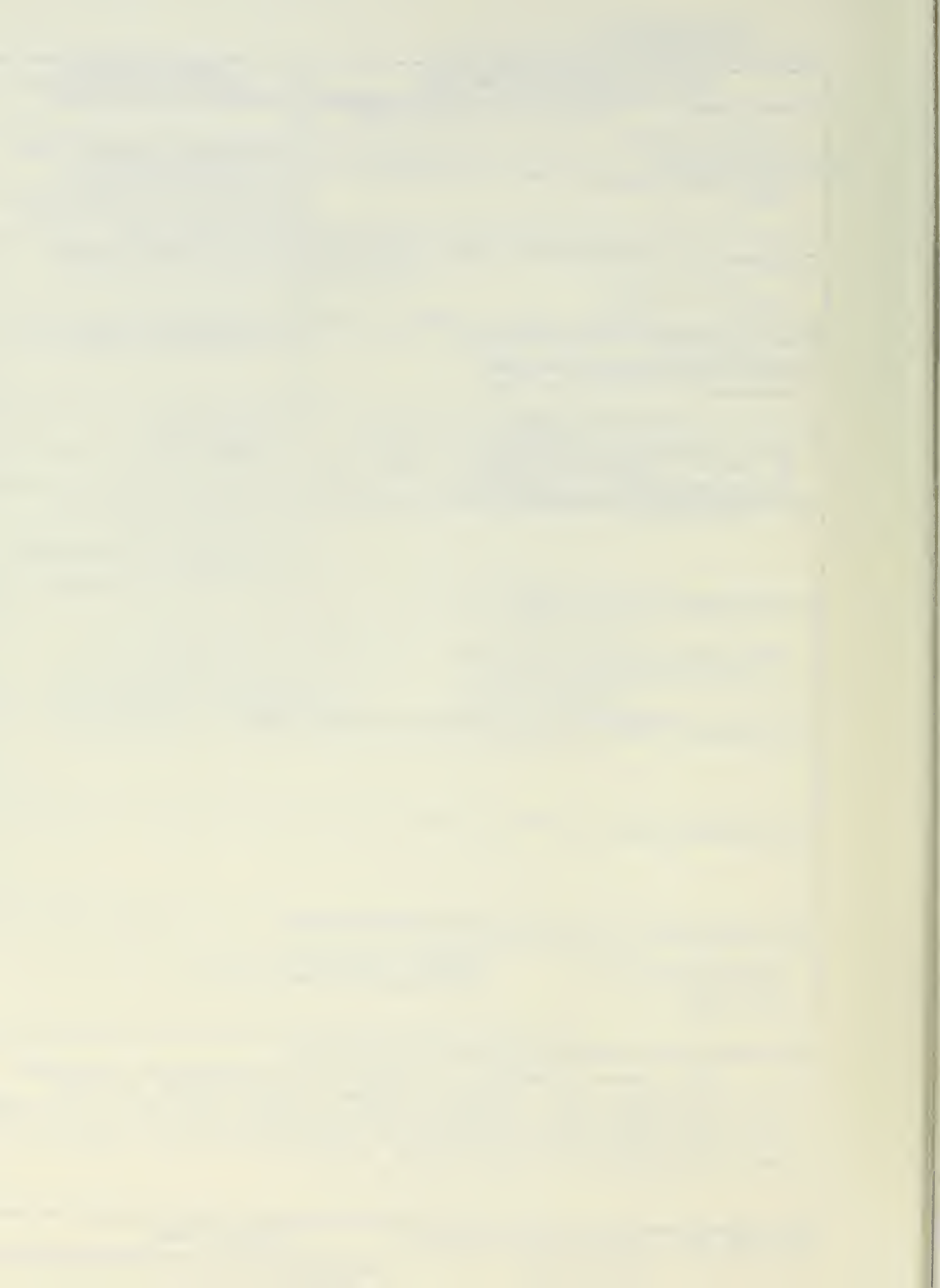
Jack R. Borsting
Provost

The work reported herein was supported by the Microwave Technology Branch (Code 2330), Naval Electronics Laboratory Center, San Diego, California.

Reproduction of all or part of this report is authorized.

This report was prepared by:

| REPORT DOCUMENTATION PAGE | | READ INSTRUCTIONS BEFORE COMPLETING FORM |
|---|-----------------------|--|
| 1. REPORT NUMBER NPS-62Ko77031A | 2. GOVT ACCESSION NO. | 3. RECIPIENT'S CATALOG NUMBER |
| 4. TITLE (and Subtitle) DIELECTRIC LOADED FINNED WAVEGUIDE STUDY | | 5. TYPE OF REPORT & PERIOD COVERED Final Report 1 Jan 77 - 31 Mar 77 |
| | | 6. PERFORMING ORG. REPORT NUMBER |
| 7. AUTHOR(s) Jeffrey B. Knorr | | 8. CONTRACT OR GRANT NUMBER(s) |
| 9. PERFORMING ORGANIZATION NAME AND ADDRESS Naval Postgraduate School Monterey, California 93940 | | 10. PROGRAM ELEMENT, PROJECT, TASK AREA & WORK UNIT NUMBERS |
| 11. CONTROLLING OFFICE NAME AND ADDRESS Naval Electronics Laboratory Center Microwave Technology Branch, Code 2330 San Diego, CA | | 12. REPORT DATE March 1977 |
| | | 13. NUMBER OF PAGES |
| 14. MONITORING AGENCY NAME & ADDRESS (if different from Controlling Office) | | 15. SECURITY CLASS. (of this report) Unclassified |
| | | 15a. DECLASSIFICATION/DOWNGRADING SCHEDULE |
| 16. DISTRIBUTION STATEMENT (of this Report) Approved for public release; distribution unlimited. | | |
| 17. DISTRIBUTION STATEMENT (of the abstract entered in Block 20, if different from Report) | | |
| 18. SUPPLEMENTARY NOTES | | |
| 19. KEY WORDS (Continue on reverse side if necessary and identify by block number) Shielded slotline Ridged Waveguide Microslotline Inhomogeneous Waveguide Fin Line | | |
| 20. ABSTRACT (Continue on reverse side if necessary and identify by block number) This report presents an analysis of rectangular waveguide with centered, zero thickness ridges (fins) backed by a dielectric substrate. Design curves are given for the 26.5-40 GHz and 40-60 GHz waveguide bands for the case where the dielectric has a thickness of 5 mils and $\epsilon_r = 2.2$. | | |



LIST OF FIGURES

- Figure 1. Rectangular waveguide loaded with zero thickness ridges backed by a dielectric slab.
- Figure 2. Wavelength ratio λ'/λ vs normalized frequency D/λ for slotline with $\epsilon_r = 2.2$.
- Figure 3. Characteristic Impedance Z_0 vs normalized frequency D/λ for slotline with $\epsilon_r = 2.2$.
- Figure 4. Cutoff wavelength λ_c/a vs. slot width W/b for a rectangular waveguide with a centered, zero thickness ridge and $b/a = 0.5$.
- Figure 5. High frequency limit of voltage-power impedance $Z_{0\infty}$ vs normalized slot width W/b for a rectangular waveguide with a centered, zero thickness ridge and $b/a = 0.5$.
- Figure 6. Dielectric slab loaded rectangular waveguide.
- Figure 7. Wavelength ratio λ'/λ vs frequency for a K_a band (26.5 - 40 GHz) waveguide loaded with a dielectric slab having $\epsilon_r = 2.2$, $d_1 = a/2$, $a = .280$ inches.
- Figure 8. Wavelength ratio λ'/λ vs frequency for a U band (40-60 GHz) waveguide loaded with a dielectric slab having $\epsilon_r = 2.2$, $d_1 = a/2$, $a = .188$ inches.
- Figure 9. Characteristic impedance Z_0 and wavelength ratio λ'/λ vs normalized frequency D/λ for a shielded slotline with $b/D = 11$, $a/D = 17$, $\epsilon_r = 20$, slab centered in shield.

- Figure 10. Effective dielectric constant vs. normalized slot width W/D for a slot line with $\epsilon_r = 2.2$.
- Figure 11. Normalized wavelength λ'/λ vs normalized frequency D/λ for shielded slotline and fin line with $a = .280$ inches, $b = .140$ inches, $D = .010$ inches, $W = .018$ inches, $\epsilon_r = 2.2$.
- Figure 12. Normalized wavelength λ'/λ vs normalized frequency D/λ for shielded slotline with $a/D = 17$, $b/D = 11$, $\epsilon_r = 20$.
- Figure 13. Normalized wavelength λ'/λ vs frequency for K_a band shielded slotline with $a = .280$ inches, $b = .140$ inches, $D = .005$ inches, $\epsilon_r = 2.2$.
- Figure 14. Normalized wavelength λ'/λ vs frequency for U band shielded slotline with $a = .188$ inches, $b = .094$ inches, $D = .005$ inches, $\epsilon_r = 2.2$.
- Figure 15. Normalized wavelength λ'/λ vs normalized slot width W/b for K_a band fin line.
- Figure 16. Normalized wavelength λ'/λ vs normalized slot width W/b for U band fin line.
- Figure 17. Normalized wavelength λ'/λ vs frequency for K_a band fin line with $D = .005$ inches.
- Figure 18. Normalized wavelength λ'/λ vs frequency for U band fin line with $D = .005$ inches.
- Figure 19. Impedance vs normalized frequency $2\pi a/\lambda$ for a slab loaded rectangular waveguide. $\epsilon_r = 2.2$, slab centered (from ref. [6]).

Figure 20. Characteristic Impedance Z_{ov} vs frequency for open boundary slotline, shielded slotline and ridged waveguide.

Figure 21. Characteristic impedance vs frequency for slotline and ridged waveguide in K_a band.

Figure 22. Characteristic impedance vs frequency for K_a band ridged waveguide.

Figure 23. Characteristic impedance vs frequency for U band ridged waveguide.

LIST OF TABLES

Table 1. Parameters for calculation of K_a band fin line wavelength ($a = .280$ inches, $b = .140$ inches, $D = .005$ inches, $\epsilon_r = 2.2$).

Table 2. Parameters for calculation of U band fin line wavelength ($a = .188$ inches, $b = .094$ inches, $D = .005$ inches, $\epsilon_r = 2.2$).

Table 3. Parameters for calculation of K_a band and U band ridged waveguide impedance ($b/a = .5$).

TABLE OF CONTENTS

Abstract

List of Figures

List of Tables

1.0 Introduction

2.0 Related Work

2.1 Unshielded Slotline

2.2 Ridged Rectangular Waveguide

2.3 Dielectric Slab Loaded Rectangular Waveguide

2.4 Fin Line

2.5 Shielded Slotline

3.0 Fin Line Wavelength

4.0 Fin Line Characteristic Impedance

5.0 Conclusions

Appendix A

References

Distribution List

1.0 Introduction

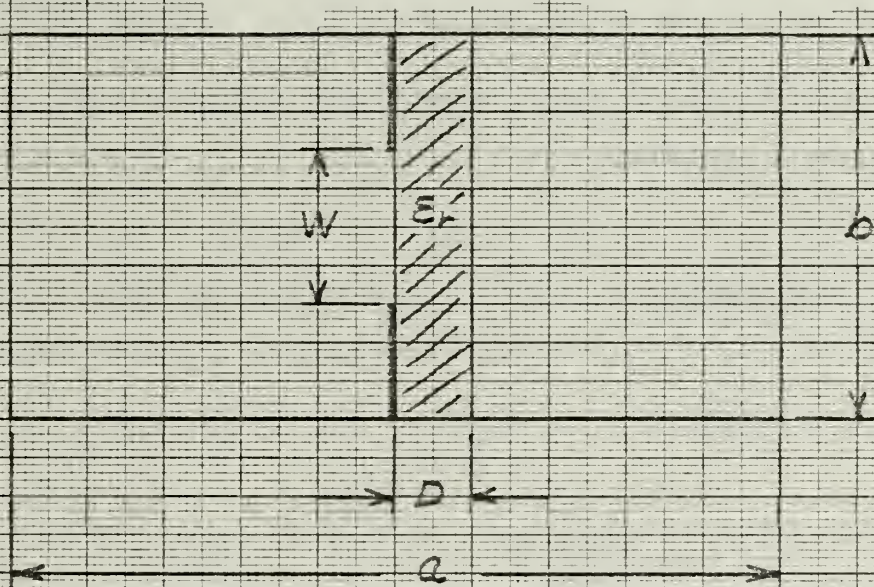
Over the years, many different types of waveguiding structures have been proposed for various uses at microwave and millimeter wave frequencies. One of these structures, the rectangular waveguide loaded with fins and a dielectric slab has recently been proposed for use in building millimeter wave integrated circuits [1]. The attributes of this structure and some experimental results have been presented in ref. [1]. The structure is shown in Figure 1.

At millimeter wave frequencies, Rogers Duroid 5880 ($\epsilon_r = 2.2$) has been found to be a particularly attractive dielectric. The purpose of this report is to present a theoretical analysis of the above described waveguide structure and to present design curves for such structures when loaded with 5 mil thickness Duroid in the 26.5-40 GHz and 40-60 GHz bands.

2.0 Related Work

The structure shown in Figure 1 is interesting in that it may be viewed in various ways depending upon the value of W/b , the ratio of slot width to waveguide height. For small values of W/b and W/D the structure may be appropriately viewed as a slotline with a rectangular shield. For values of $W/b \rightarrow 1$ the structure is more easily viewed as a ridged waveguide loaded with dielectric. Finally, for $W/b = 1$, we have a dielectric slab loaded waveguide. Each of these substructures has been studied previously. Since the analysis of the structure

Figure 1 Rectangular waveguide loaded with zero thickness ridges backed by a dielectric slab.



shown in Figure 1 is based upon the studies of these substructures these related investigations will be reviewed briefly.

2.1 Unshielded Slotline

Unshielded slotline has been studied by Cohn [2] and by Knorr and Kuchler [3]. The analysis presented in reference [3] allows the wavelength and characteristic impedance to be determined for both single and coupled slots. The solutions are found by applying the method of moments in the transform domain where the Fourier transform of the slot field is expanded in a set of basis functions. It is found that for narrow slots, a one term expansion of E_x is usually adequate. Computer time increases rapidly if multi-term expansions are required as would be the case for wide slots.

The computer program described in ref. [3] was used to produce the curves shown in Figures 2 and 3. The impedance shown in Figure 3 is defined by the relation

$$Z_0 = \frac{V_0^2}{2P_{AVG}} \quad (1)$$

where

$$V_0 = - \int_{\text{slot}} E_x dx \quad P_{AVG} = \frac{1}{2} R_e \iint \bar{E}_x \bar{H}^* \cdot \bar{a}_z da \quad (2)$$

A curious feature of these curves is the crossovers observed for different values of W/D . This will be commented upon further in section 4.0, Fin Line Impedance.

Figure 2 Wavelength ratio λ'/λ vs normalized frequency D/λ for slotline with $\epsilon_r = 2.2$.

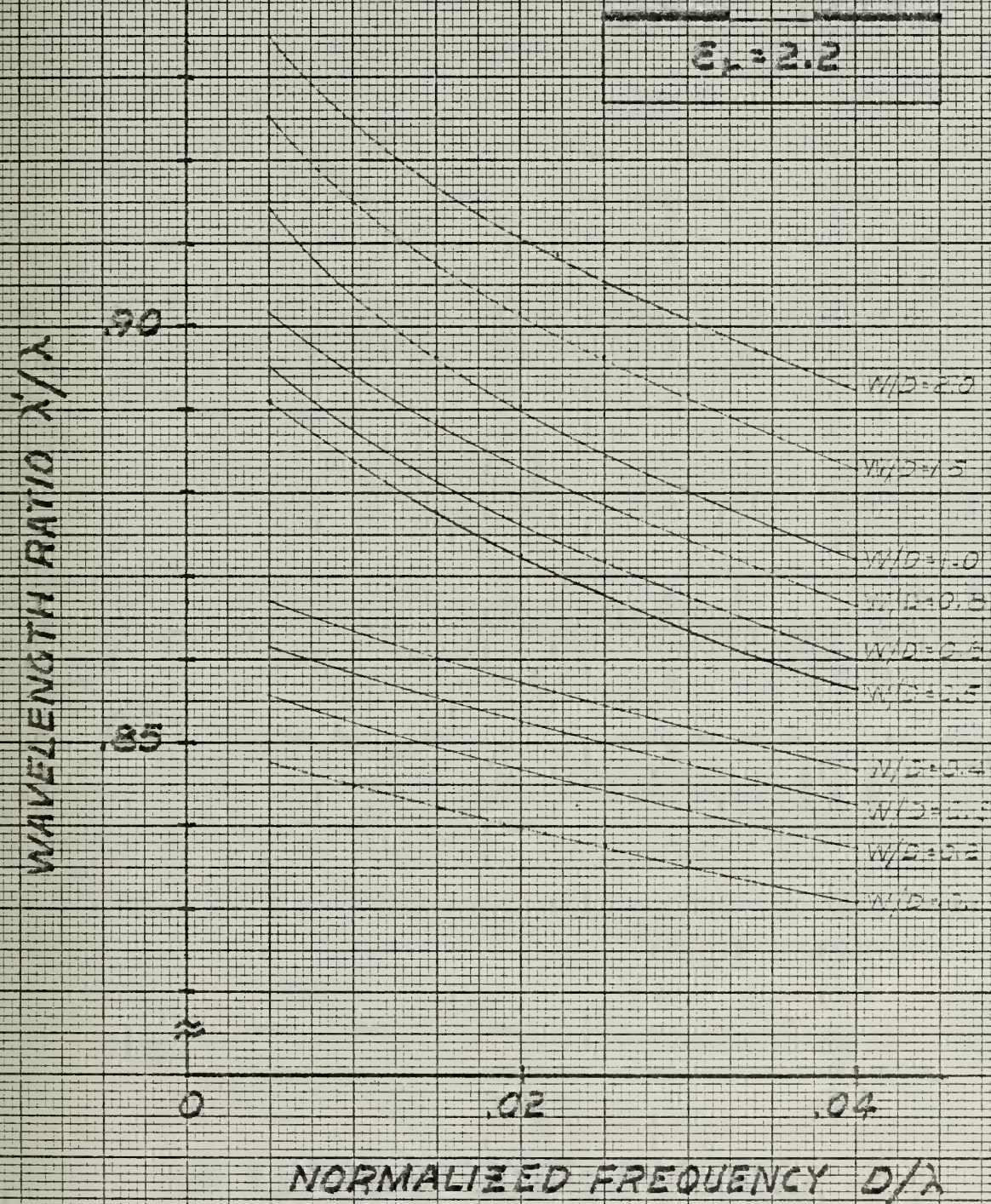
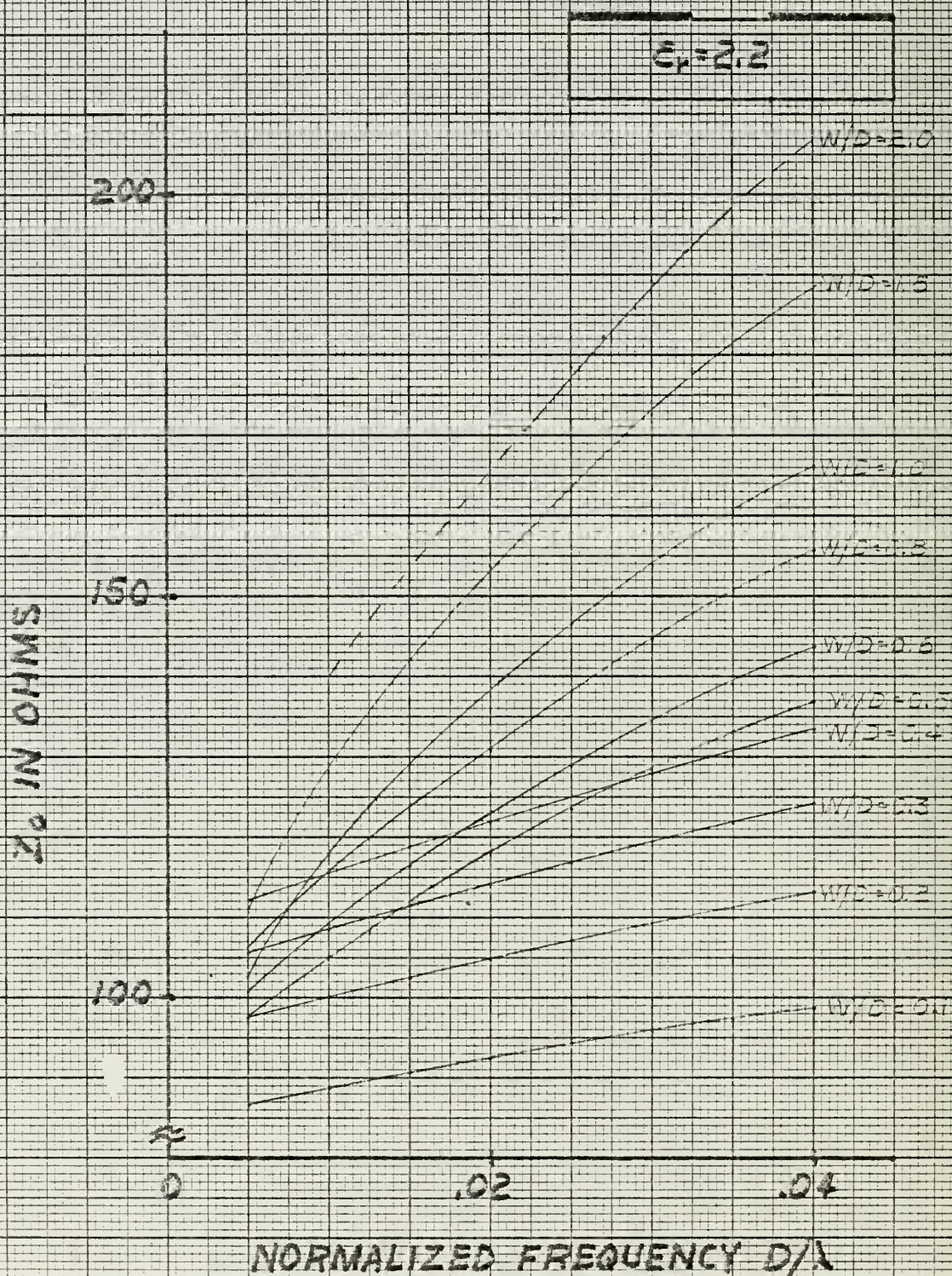


Figure 3 Characteristic impedance Z_0 vs normalized frequency D/λ for slotline with $\epsilon_r = 2.2$.



2.2 Ridged Waveguide

The design of ridged waveguide has been treated by Hopfer [4]. Of particular interest in this study is the curve of cutoff wavelength for a waveguide with $b/a = .5$ and a centered, zero thickness ridge. This information is presented in Figure 4. With this information one may calculate the normalized wavelength ratio for $0 \leq W/b \leq 1$ as

$$\frac{\lambda'}{\lambda} = \frac{1}{\left[1 - \left(\frac{\lambda}{\lambda_c}\right)^2\right]^{\frac{1}{2}}} \quad (3)$$

where λ is the free space wavelength and λ_c is found from Figure 4. The ridged waveguide corresponds to the structure of interest in this study (Figure 1.) except for the absence of the dielectric slab.

Lagerlöf has also studied ridged waveguide and has presented design curves [5] valid for a wide range of parameters subject to a zero thickness ridge restriction. The curves presented in [5] allow the high frequency limit impedance, $Z_{ov\infty}$, defined on a voltage-power basis to be found. Figure 5 shows a plot of $Z_{ov\infty}$ vs W/b for the case $b/a = 0.5$ as determined from Lagerlöf's curves. Having found $Z_{ov\infty}$ for the correct value of $0 \leq W/b \leq 1$ one calculates the impedance at any frequency as

$$Z_{ov} = \frac{Z_{ov\infty}}{\left[1 - \left(\frac{\lambda}{\lambda_c}\right)^2\right]^{\frac{1}{2}}} \quad (4)$$

Again, this corresponds to the structure of interest in this study

Figure 4. Cutoff wavelength λ_c/a vs. slot width W/b for a rectangular waveguide with a centered zero thickness ridge and $b/a = 0.5$.

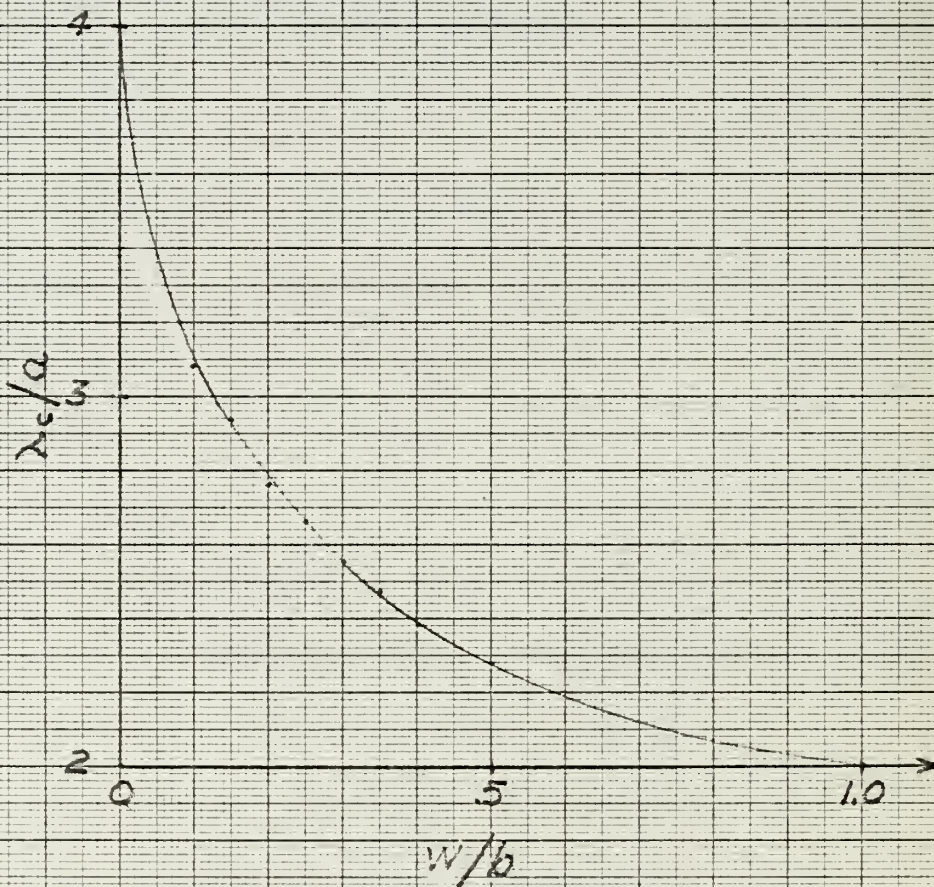
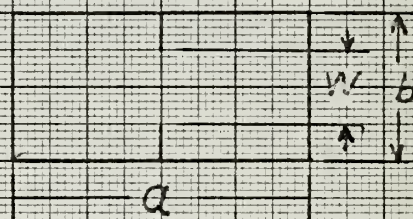
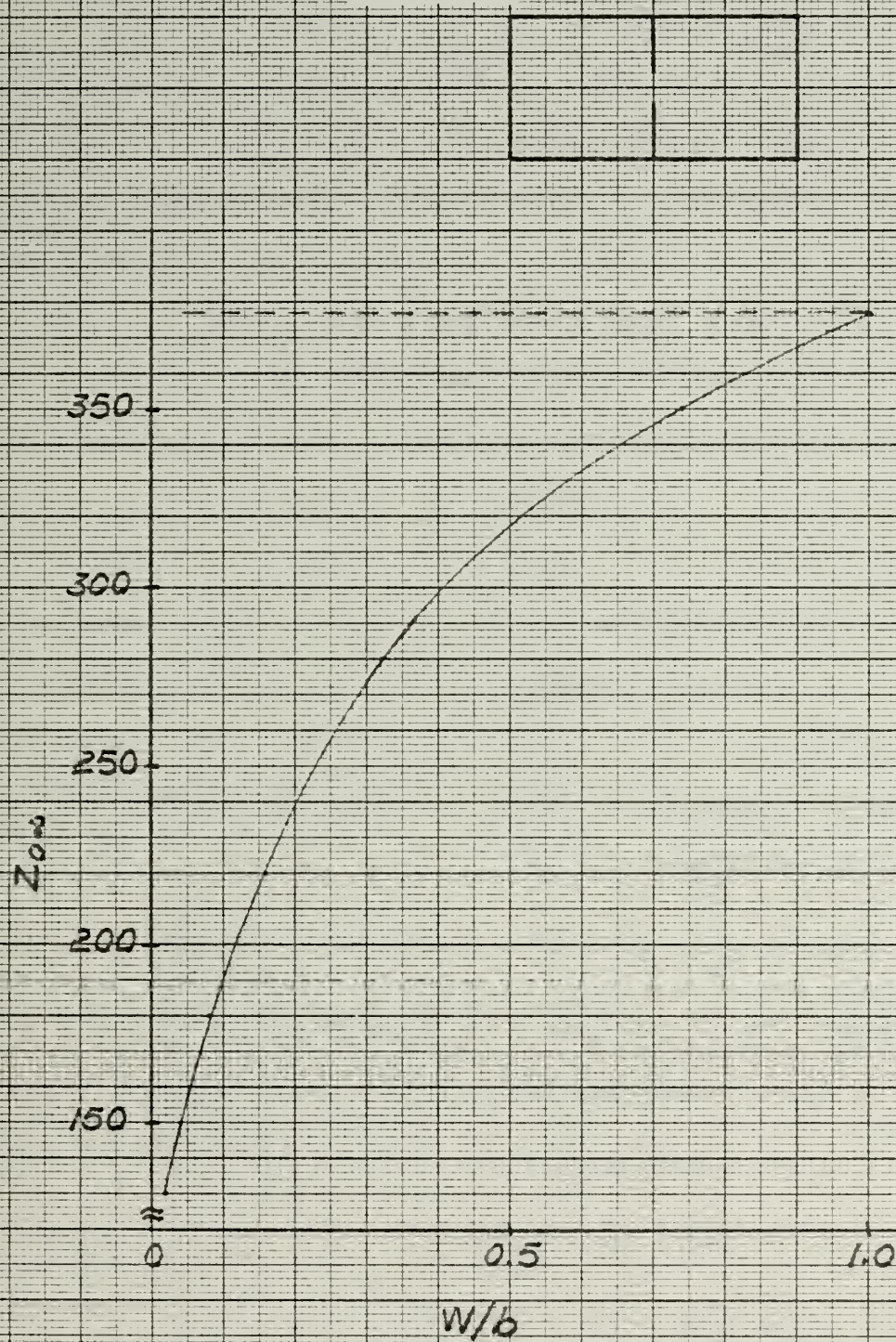


Figure 5 High frequency limit of voltage-power impedance $Z_{0\infty}$ vs normalized frequency slot width W/b for a rectangular waveguide with a centered, zero thickness ridge and $b/a = 0.5$.



except for the absence of the dielectric substrate. Ridged waveguide is therefore a substructure of fin line which results when $D = 0$.

2.3 Slab Loaded Waveguide

For the case of $W/b = 1$, the structure of Figure 1. becomes another fin line substructure, the dielectric slab loaded rectangular waveguide. The dielectric slab loaded rectangular waveguide has been studied in considerable detail by Vartanian, et al. [6]. This paper presents a wide range of information of general interest which will be referred to again in section 4.0. Since Vartanian gives results only for $\epsilon_r = 2.5, 9.0$ and 16.0 the results presented here were obtained using the transverse resonance procedure [7] which is found by writing the field equations for an exact solution of the problem, applying boundary conditions at the air-dielectric interfaces and thereby obtaining the determinantal equation for the system. With reference to Figure 6, the wavelength ratio is found by determining that value which satisfies

$$B_\ell + B_r = 0 \quad (5)$$

where

$$B_\ell = -h \cot(hD + \theta) \quad (6a)$$

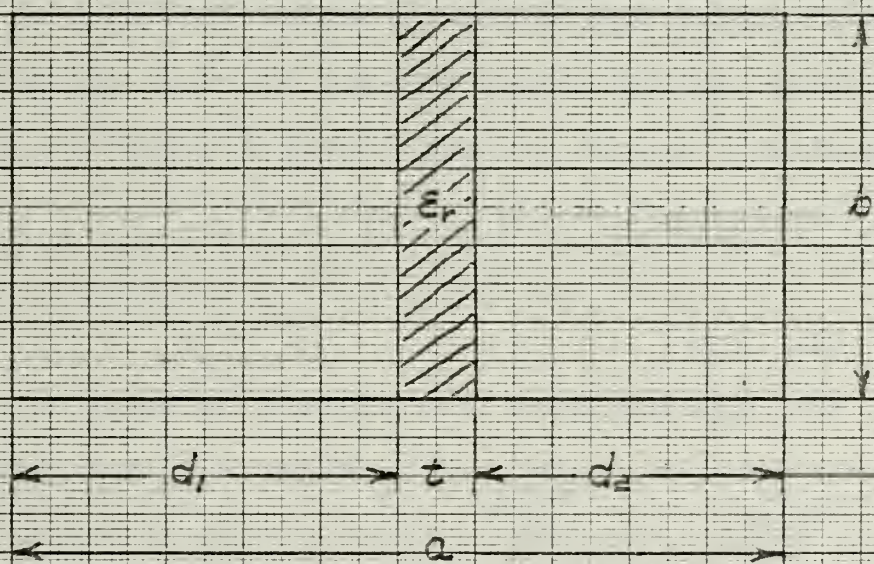
$$B_r = -\ell \cot(\ell d_2) \quad (6b)$$

$$\theta = \tan^{-1} \left(\frac{h}{\ell} \tan \ell d_1 \right) \quad (6c)$$

$$h^2 = \left(\frac{2\pi}{\lambda} \right)^2 \left[1 - \left(\frac{\lambda}{\lambda_1} \right)^2 \right] \quad (6d)$$

$$\ell^2 = \left(\frac{2\pi}{\lambda} \right)^2 \left[\epsilon_r - \left(\frac{\lambda}{\lambda_1} \right)^2 \right] . \quad (6e)$$

Figure 6 Dielectric slab loaded rectangular waveguide.



Equation (5) was solved numerically by searching iteratively for the value of λ'/λ satisfying equation (5). The results are presented in Figures 7. and 8. The machine used for these calculations was a Wang 500 and the program is given in Appendix A. The wavelength ratios were determined to within .005 which gives an accuracy better than $\frac{1}{2}\%$ in all cases.

The admittance formulation, equation (5), was used rather than the impedance formulation to achieve numerical stability. For the position and thickness of the slab which is of interest here, the susceptances are small and $B_\ell + B_r$ goes smoothly through zero. The impedance formulation $X_\ell + X_r = 0$ results in taking the difference between two very large quantities with a resultant violent and unreliable fluctuation through zero in the neighborhood of the correct λ'/λ .

2.4 Fin Line

Fin line has been investigated by Meier [1]. One difference between the structure used by Meier and that shown in Figure 1. is the use of r.f. choking vice direct electrical contact between the shield and the fins. Meier's work was primarily experimental in nature. He showed that the expression

$$\lambda'/\lambda = \frac{1}{\left[k_e - \left(\frac{\lambda}{\lambda_c} \right)^2 \right]^{\frac{1}{2}}} \quad (7)$$

provided a good fit ($\pm 2\%$) to K_a band experimental data. The effective dielectric constant, k_e , was determined by measurement at any one frequency and λ_c is the cutoff wavelength of ridged

Figure 7 Wavelength ratio λ'/λ vs frequency for
a K_a band (26.5 - 40 GHz) waveguide loaded
with a dielectric slab having $\epsilon_r = 2.2$,
 $d_1 = a/2$, $a = .280$ inches.

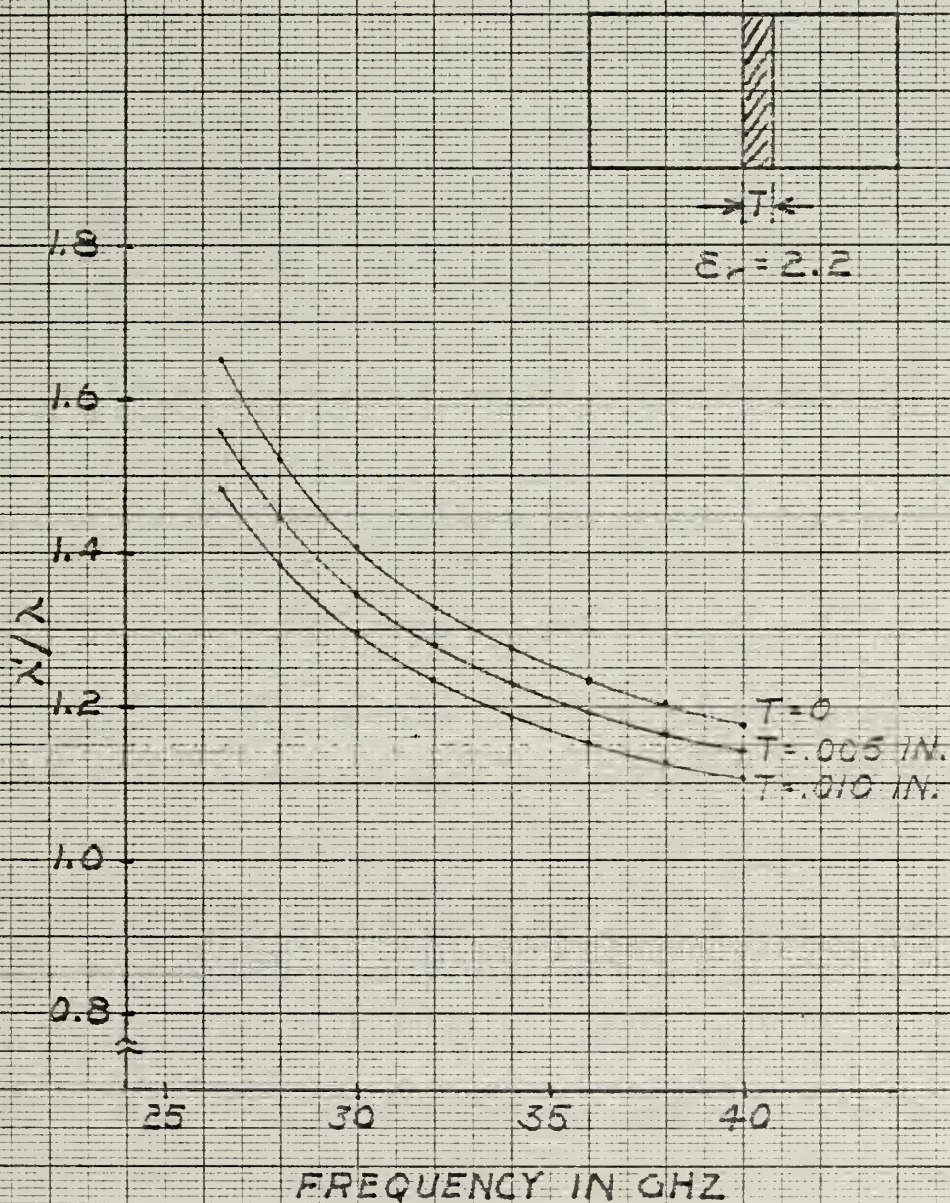
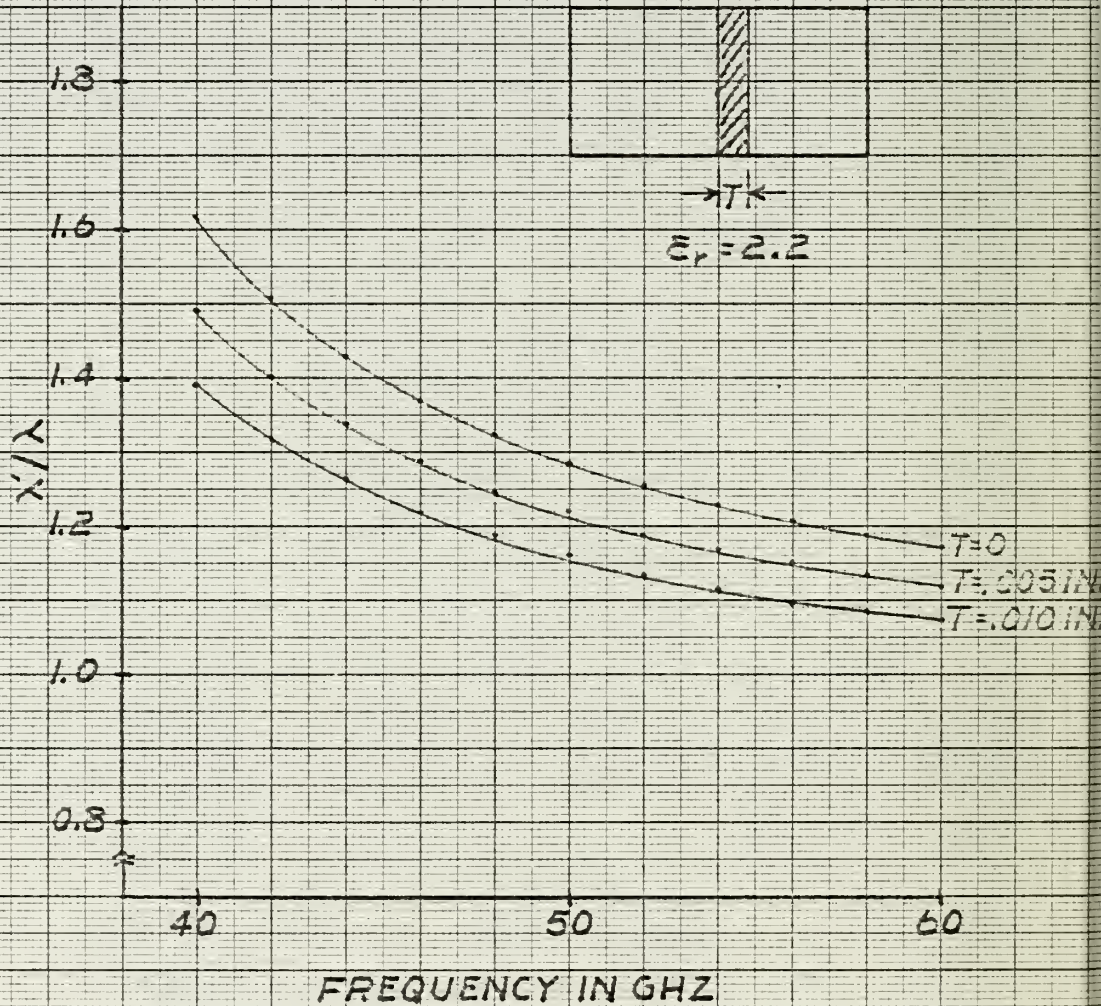


Figure 8 Wavelength ratio λ'/λ vs frequency for a U band (40 - 60 GHz) waveguide loaded with a dielectric slab having $\epsilon_r = 2.2$, $d_1 = a/2$, $a = .188$ inches.



waveguide (no dielectric) as found from Figure 4.

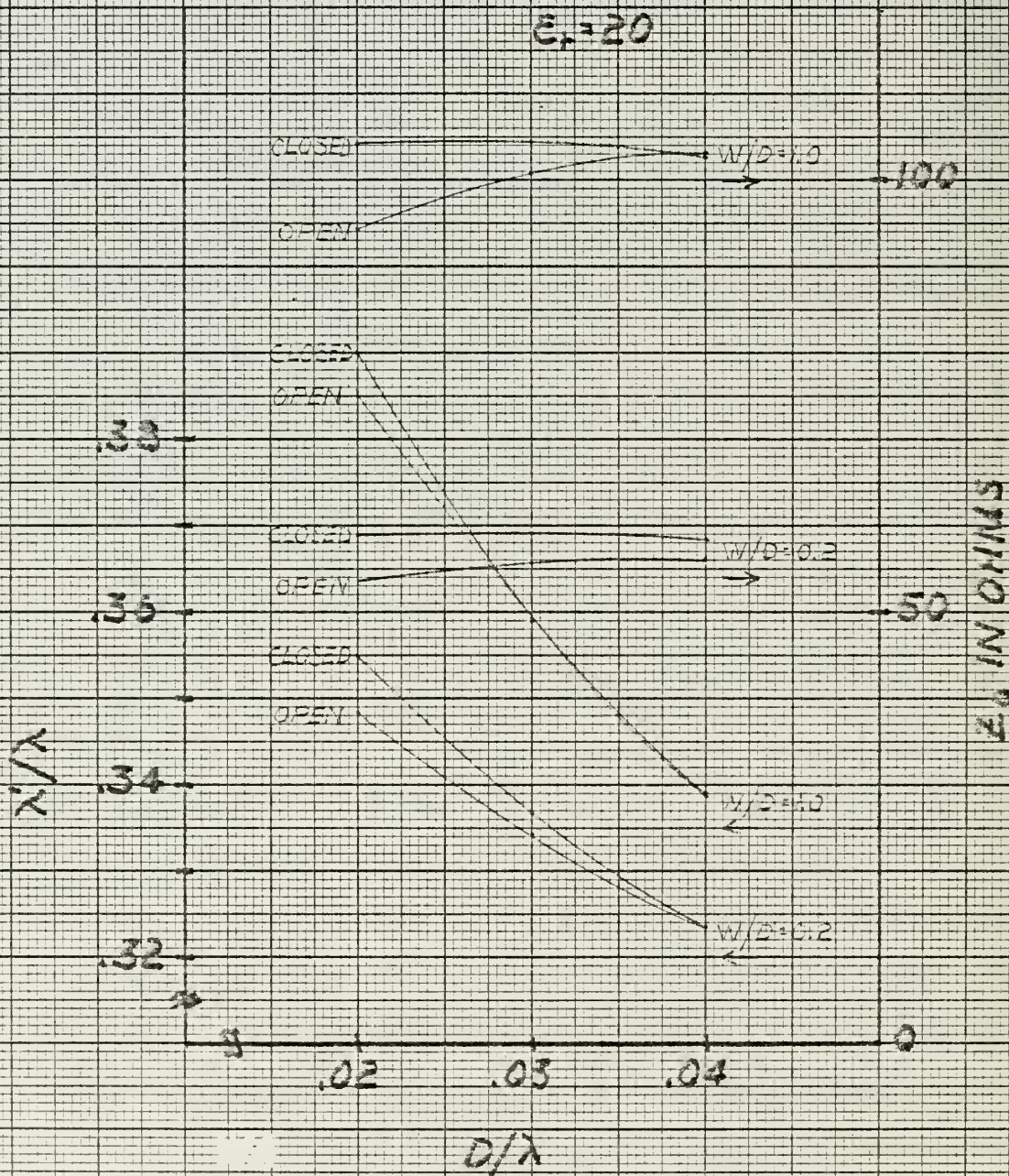
Meier made no impedance measurements.

2.5 Shielded Slotline

Shielded slotline has been analyzed by Kuchler [8] using a technique similar to that described in [3]. Solutions are obtained by computer as in [3]. Some results obtained using the computer program described in [8] are shown in Figure 8. Also shown are results for an unshielded slotline as obtained using the program described in reference [3]. The significant feature is that at higher frequencies where the wave is tightly bound to the slot and where there is little interaction with the shield the results for the shielded line converge to those for the unshielded line. It is also to be noted that both wavelength and characteristic impedance are increased by the presence of the shield.

Ideally, it should have been possible to obtain the characteristics of the structure shown in Figure 1 for small values of W/b and W/D using the method of [8]. However, the computer program generated overflows and errors for the range of parameters (ϵ_r , shield size, etc.) of interest in this study. The computer program is being rewritten at this time but this is a major undertaking which could not be completed in time to provide results for this study. Therefore, the results shown in Figure 9 were used for two purposes:

Figure 9 Characteristic impedance Z_0 and wavelength ratio λ'/λ vs normalized frequency D/λ for a shielded slotline with $b/D = 11$, $a/D = 17$, $\epsilon_r = 20$, slab centered in shield.



1. to determine the effects of the shield as noted previously,
2. to check the approximate approach developed in section 3.0 of this report.

For the purposes of this report, slotline will imply $W/D \lesssim 2$, $W/b \lesssim .1$ whereas fin line implies $0 < W/b \leq 1$. Slotline is therefore a substructure of fin line.

3.0 Fin Line Wavelength

In this section, we will consider an approximate method of evaluating the wavelength of dielectric loaded, zero thickness double ridged waveguide as depicted in Figure 1. We will refer to this structure as fin line, keeping in mind the physical differences between the fin line built by Meier [1] and the fin line shown in Figure 1. Electromagnetically, the characteristics of the two structures should be very nearly the same. Fin line will be analyzed using a substructure approach.

Section 2.4 discussed fin line and the dispersion characteristic as given by equation (7). The view taken here is essentially the same; for small values of W/b , ϵ_r and $f \gg f_c$, the structure behaves as a ridged waveguide with effective dielectric constant determined by the slab of dielectric. Equivalently stated, the structure behaves as if filled with a homogeneous dielectric having "effective" dielectric constant less than the actual dielectric constant of the slab. Meier

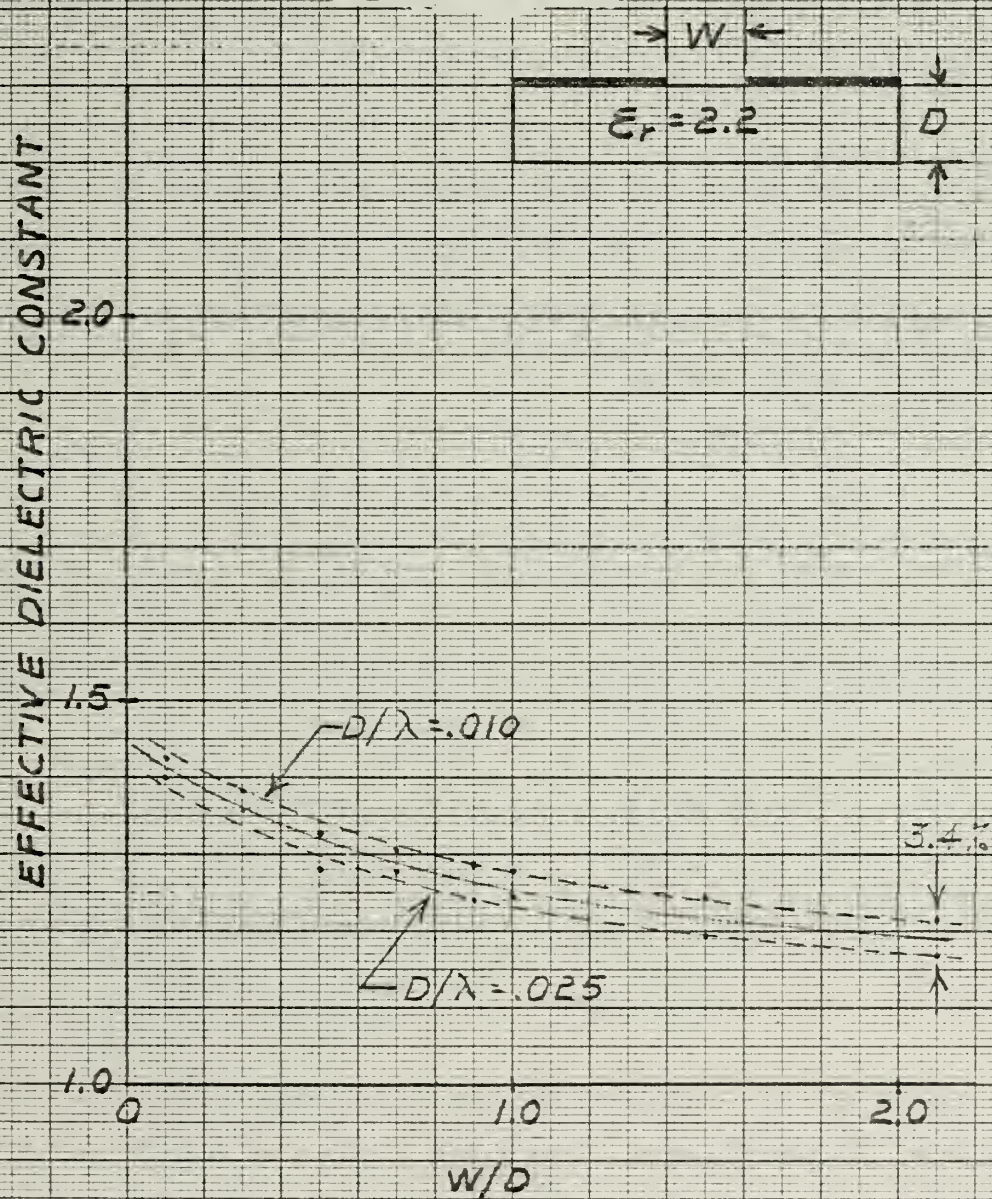
determined the "effective" dielectric constant by measurement. This is a generally undesirable approach since extensive effort would be required to develop design curves for the many possible geometries and dielectric constants of interest. Here, we take the view that the effective dielectric constant (for $W/b \lesssim 1$, $W/D \lesssim 2$) can be determined from existing open boundary slotline design curves which may be obtained by the methods discussed in section 2.1.

To substantiate this claim, the wavelength obtained by this method has been checked against data published by Meier [1] and against the theoretical curves for shielded slotline produced using Kuchler's program [8].

Figure 10 shows the effective dielectric constant, $(\lambda/\lambda')^2$, of a slotline with $\epsilon_r = 2.2$ plotted vs the normalized slot width W/D . The frequency range of interest here is 26.5-60 GHz and for a substrate thickness $D = .005$ inches, the corresponding range of D/λ is $.0112 \leq D/\lambda \leq .0254$. It can be seen from Figure 10 that the effective dielectric constant varies by less than 4% over this range of D/λ . In all subsequent calculations therefore, the average given by the solid curve in Figure 10 has been used.

Meier measured the wavelength of fin line constructed using a $D = 10$ mil substrate ($\epsilon_r = 2.2$), a K_a band waveguide shield ($a = .280$ inches, $b = .140$ inches) and fin separation $W/D = 1.8$ ($W = .018$ inches). His experimentally determined value of

Figure 10 Effective dielectric constant vs. normalized slot width W/D for a slot line with $\epsilon_r = 2.2$.



"effective" dielectric constant k_e was 1.31. His experimental data was within 2% of the curve calculated from equation (7) where k_e was taken as 1.31 and $\lambda_c = 2.15$ cm as determined from Figure 4. This curve is plotted in Figure 11 along with the curve calculated using the present method where $k_e = 1.20$ as determined from figure 10. The difference in the results is less than 5%. This seems quite reasonable considering the differences between Meier's fin line and the structure of Figure 1.

A second check on this method was made by calculating the wavelength ratio for the structure of Figure 1 for comparison with Kuchler's results, again using equation (7) which may be rewritten in the form

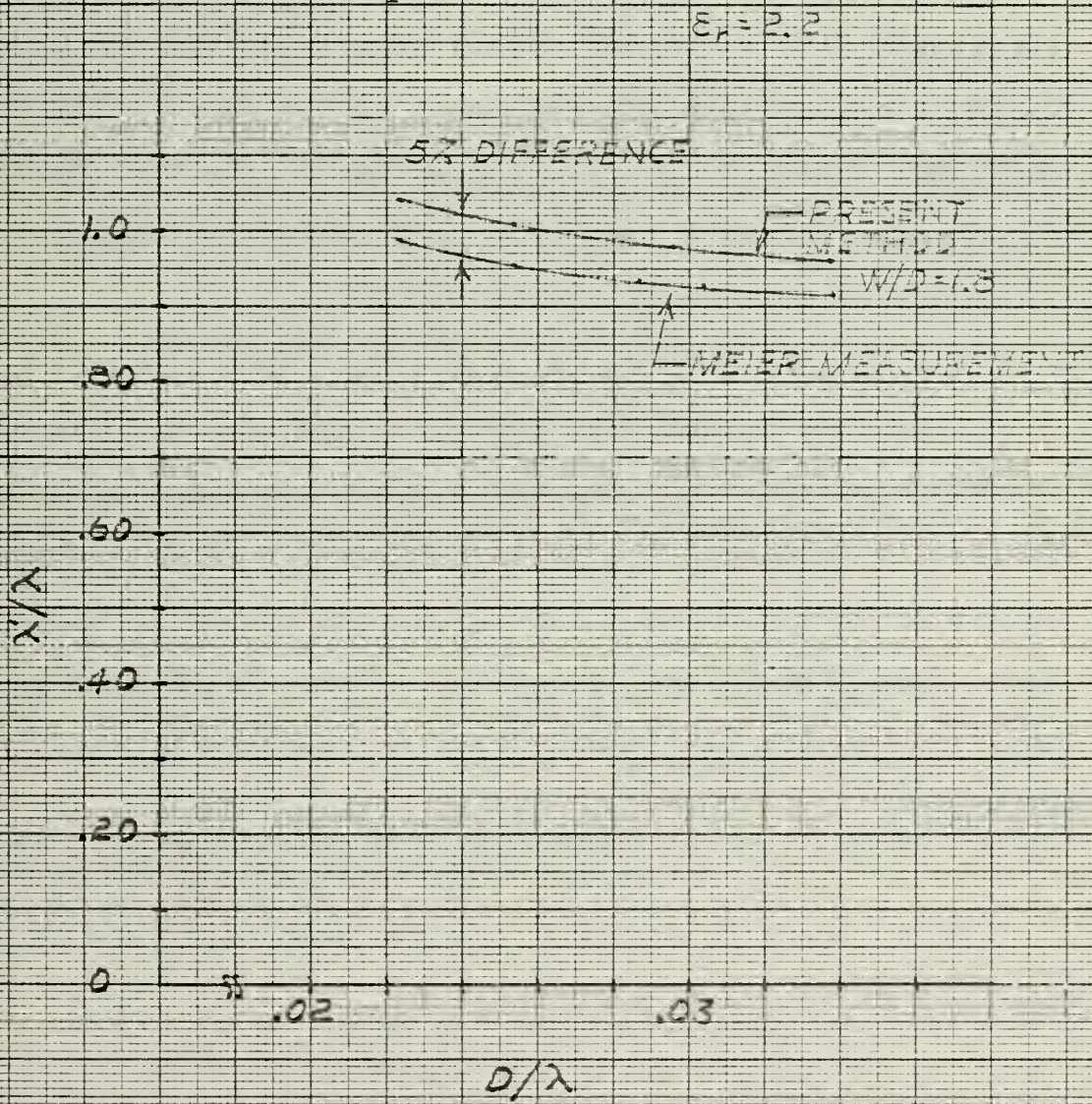
$$\left(\frac{\lambda'}{\lambda}\right)_{\text{closed}} = \frac{1}{\left[\left(\frac{\lambda'}{\lambda_{\text{open}}}\right)^2 - \left(\frac{D/\lambda_c}{D/\lambda}\right)^2 \right]^{1/2}} \quad (8)$$

Calculations were made for the following cases:

| | |
|-----------------------|-----------------------|
| 1. $b/D = 11$ | 2. $b/D = 11$ |
| $a/D = 17$ | $a/D = 17$ |
| $\epsilon_r = 20$ | $\epsilon_r = 20$ |
| $W/D = .20$ | $W/D = 1.0$ |
| $W/\lambda_c = .0134$ | $D/\lambda_c = .0173$ |

The values of D/λ_c for these two cases are determined from the curves given by Lagerlöf [5] vice Figure 4 since in this case the ratio $b/a = 11/17$. The effective dielectric constant, $k_e = (\lambda/\lambda')$ was determined from Figure 9. An "exact" value of k_e was used

Figure 11 Normalized wavelength λ'/λ vs normalized frequency D/λ for shielded slotline and fin line with $a = .280$ inches, $b = .140$ inches, $D = .010$ inches, $W = .018$ inches, $\epsilon_r = 2.2$.



in this case since there was significant variation of k_e with frequency. For $W/D = 1$, $6.7 \leq k_e \leq 8.7$ and for $W/D = 0.2$, $8.2 \leq k_e \leq 9.5$ as D/λ varied from .02 to .04. The results of these calculations are shown in Figure 12 where they are compared with the results obtained using Kuchler's shielded slotline program. The agreement is very good with the difference being 5% in the worst case.

The comparisons shown in Figures 11 and 12 involve structures with different shield aspect ratios, vastly different dielectric constants and different slot widths. The very good agreement between results obtained using this approximate method and results obtained both experimentally and numerically provides considerable confidence in the method.

Next, the method just described was used to calculate the characteristics of K_a band and U band waveguides with fins and dielectric loading. The parameters used to enter Figures 4 and 10 are given in tables 1 and 2. The values of k_e and λ_c found from these figures are also given. These parameters are then used in equation (7) to calculate the results plotted in Figures 13 and 14.

With regard to Figure 1, we now have available the following information about the structure:

1. $D = 0$, λ'/λ for all values of W/b
2. $D = .005$ inches, λ'/λ for small values of W/b
and for $W/b = 1$.

Figure 12 Normalized wavelength λ'/λ vs normalized frequency D/λ for shielded slotline with $a/D = 17$, $b/D = 11$, $\epsilon_r = 20$.

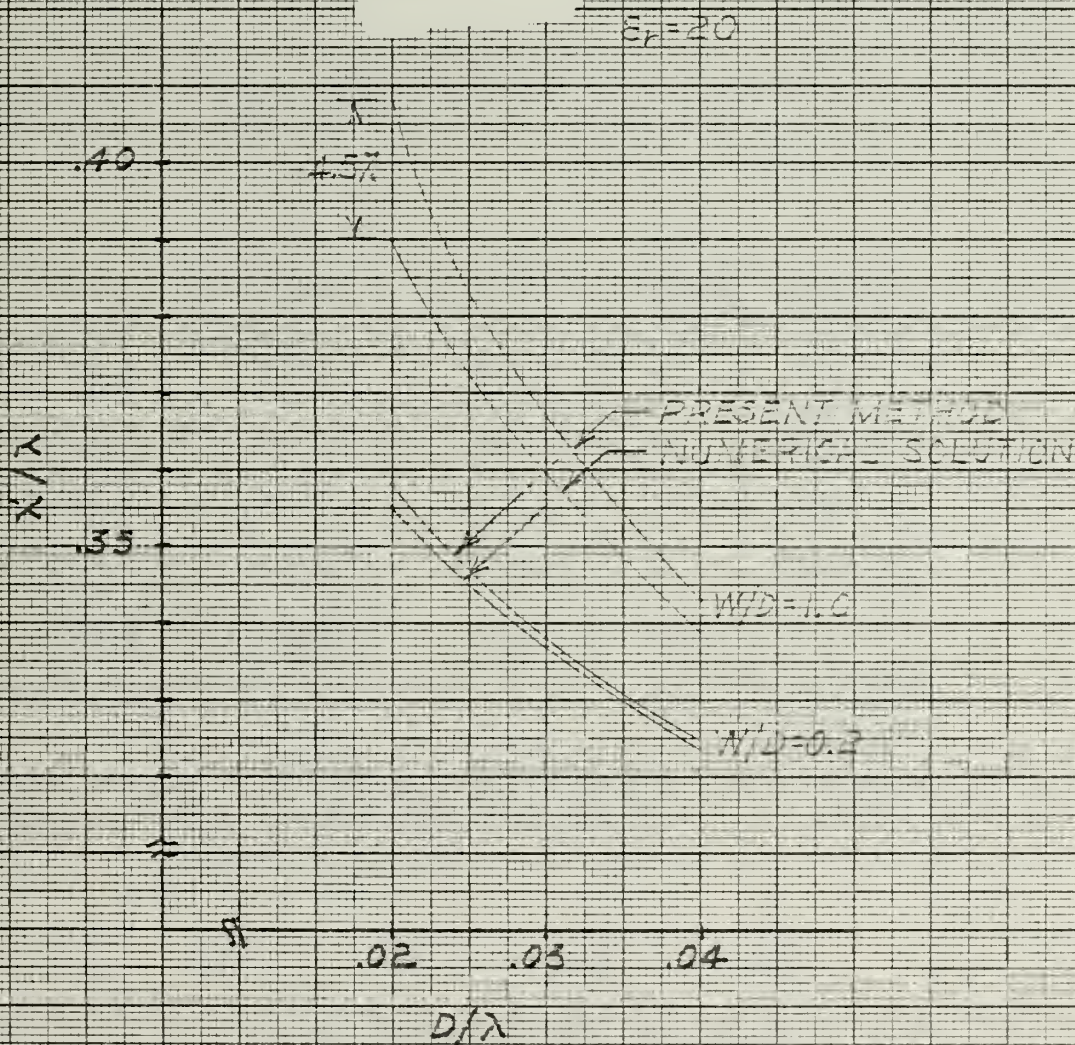


Table 1. Parameters for calculation of K_a band fin line wavelength
(a = .280 inches, b = .140 inches, D = .005 inches,
 $\epsilon_r = 2.2$).

| W(in.) | W/D | k_e^* | W/b | λ_c/a^{**} | λ_c (cm.) |
|--------|-----|---------|-------|--------------------|-------------------|
| .002 | .4 | 1.34 | .0143 | 3.70 | 2.63 |
| .004 | .8 | 1.28 | .0286 | 3.58 | 2.55 |
| .006 | 1.2 | 1.24 | .0428 | 3.44 | 2.45 |
| .008 | 1.6 | 1.21 | .0571 | 3.34 | 2.38 |
| .010 | 2.0 | 1.19 | .0714 | 3.24 | 2.30 |

Table 2. Parameters for calculation of U band fin line wavelength.
(a = .188 inches, b = .094 inches, D = .005 inches,
 $\epsilon_r = 2.2$)

| W(in.) | W/D | k_e^* | W/b | λ_c/a^{**} | λ_c (cm.) |
|--------|-----|---------|-------|--------------------|-------------------|
| .002 | .4 | 1.34 | .0213 | 3.62 | 1.73 |
| .004 | .8 | 1.28 | .0426 | 3.44 | 1.64 |
| .006 | 1.2 | 1.24 | .0638 | 3.30 | 1.56 |
| .008 | 1.6 | 1.21 | .0851 | 3.18 | 1.52 |
| .010 | 2.0 | 1.19 | .1064 | 3.07 | 1.47 |

* From Figure 10

** From Figure 4

Figure 13 Normalized wavelength λ'/λ vs frequency
for K_a band shielded slotline with
 $a = .280$ inches, $D = .005$ inches, $\epsilon_r = 2.2$.

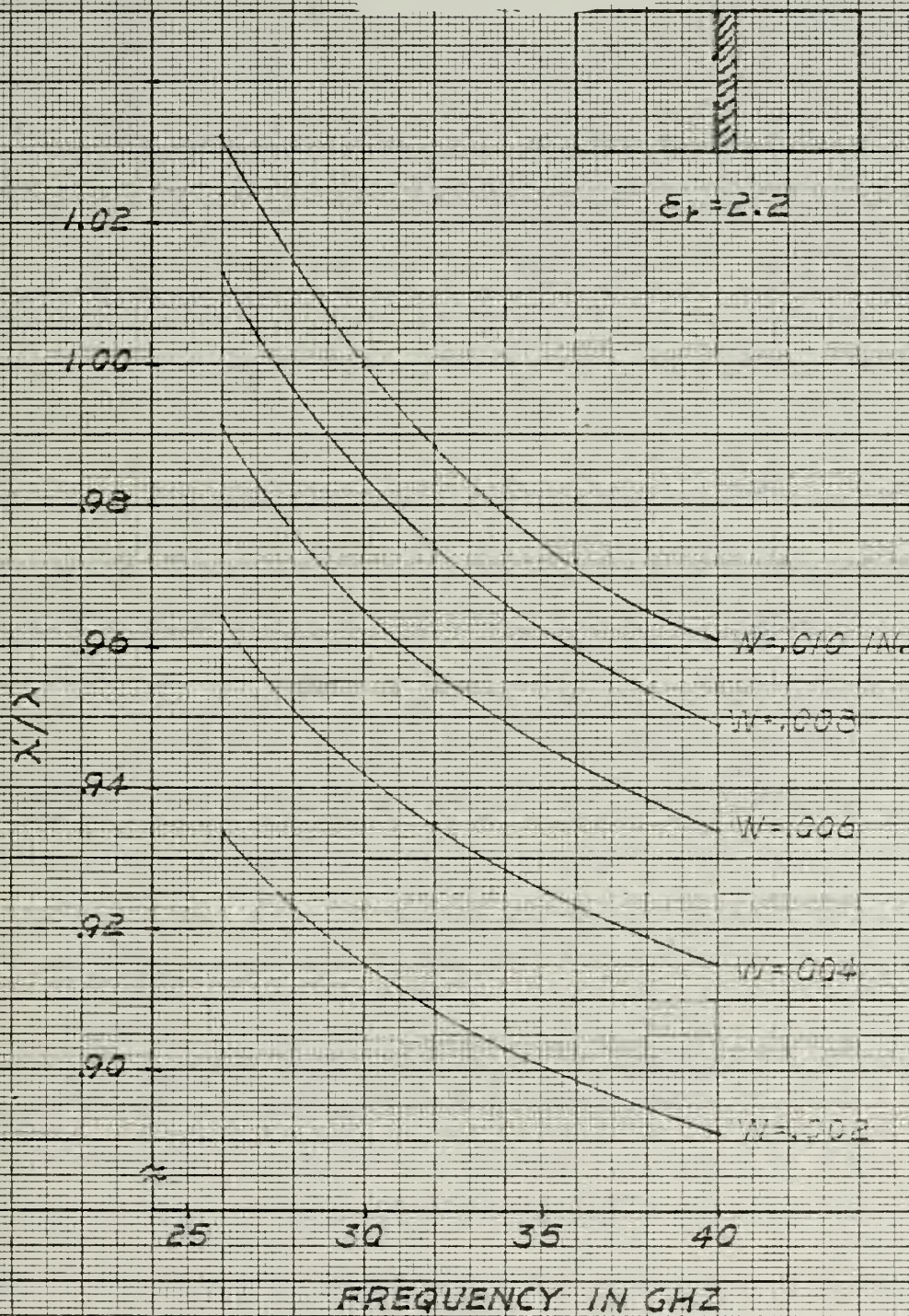
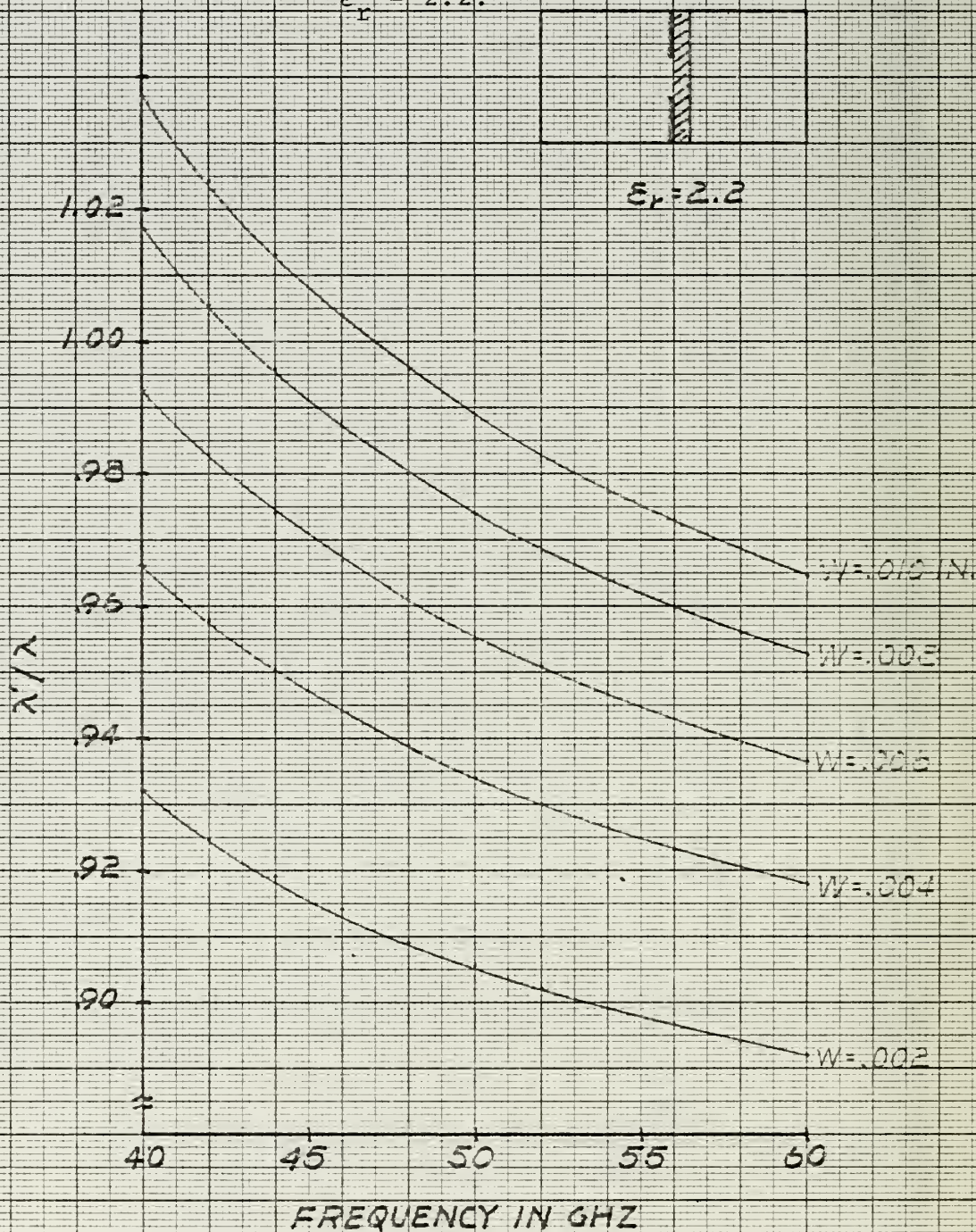


Figure 14 Normalized wavelength λ'/λ vs frequency for U band shielded slotline with $a = .1$ inches, $b = .094$ inches, $D = .005$ inches $\epsilon_r = 2.2$.



Information about λ'/λ has not been obtained for the cases $D = .005$ inches, $0.1 < W/b < 1$. However, if we plot the available information about λ'/λ vs W/b for a few different frequencies as is shown in Figures 15 and 16 it is clear that we can easily obtain the missing portion of the solution by extrapolation between the approximate solution for small values of W/b and the exact solution for $W/b = 1$. The extrapolation is shown by the dashed curves in the figures. Figures 17 and 18 follow immediately from Figures 15 and 16. These figures present the desired result for intermediate values of W/b ($.1 < W/b < 1$).

In summary, Figures 13, 14, 17 and 18 present λ'/λ vs frequency for the entire range of values of W/b . The error in these curves should be on the order of 5% for small values of W/b and decreasing to $\frac{1}{2}\%$ for $W/b = 1.0$. In applying the information in these figures one should keep in mind that any physical differences between the structure analyzed here (Figure 1) and any structure actually constructed (such as Meier's fin line) may result in discrepancies between this theory and measured data.

4.0 Characteristic Impedance

The characteristic impedance of the structure of Figure 1 has not been found. In general, the author has found in solving related problems that the characteristic impedance of a structure supporting a hybrid field generally behaves in ways that one would not expect [3], [9]. This makes it difficult to employ

Figure 15. Normalized wavelength λ'/λ vs normalized slot width W/b for K_a band fin line.

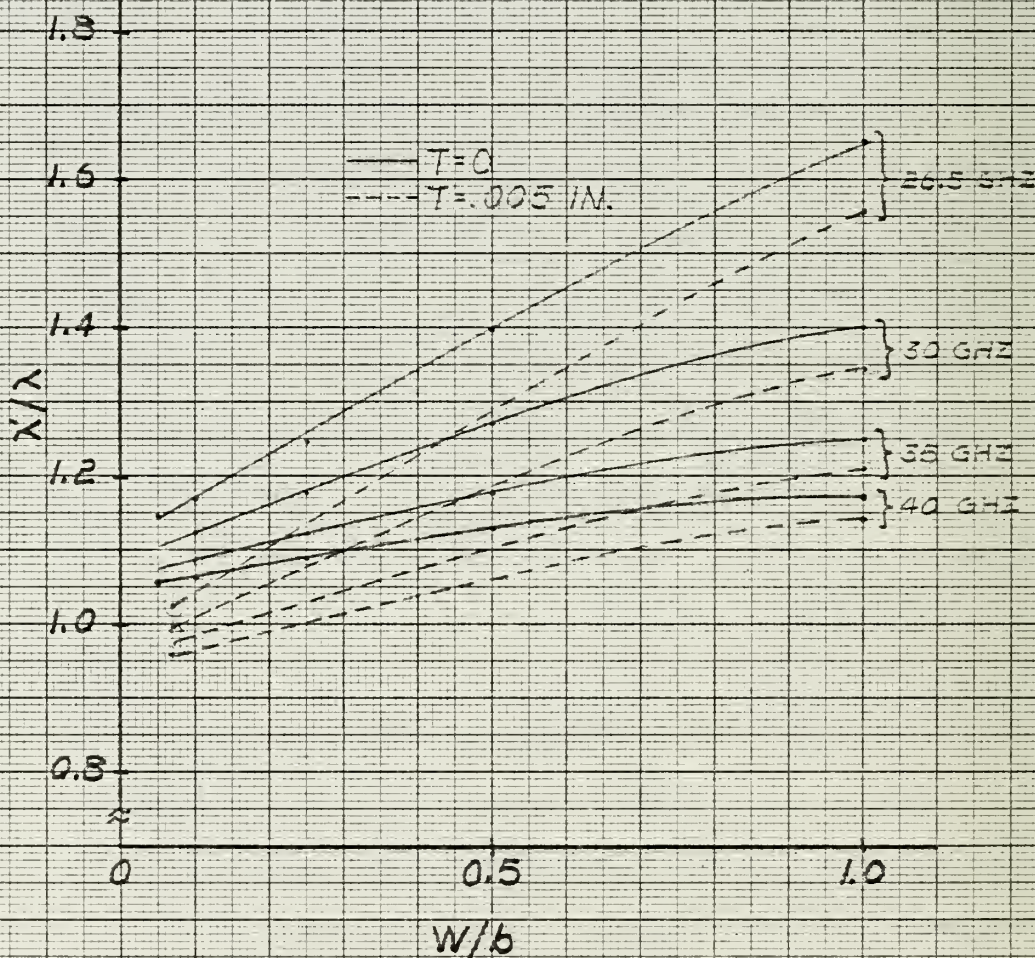
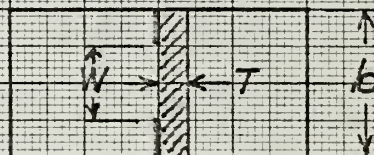


Figure 16 Normalized wavelength λ'/λ vs normalized slot width W/b for U band fin line.



$\epsilon_r = 2.2$

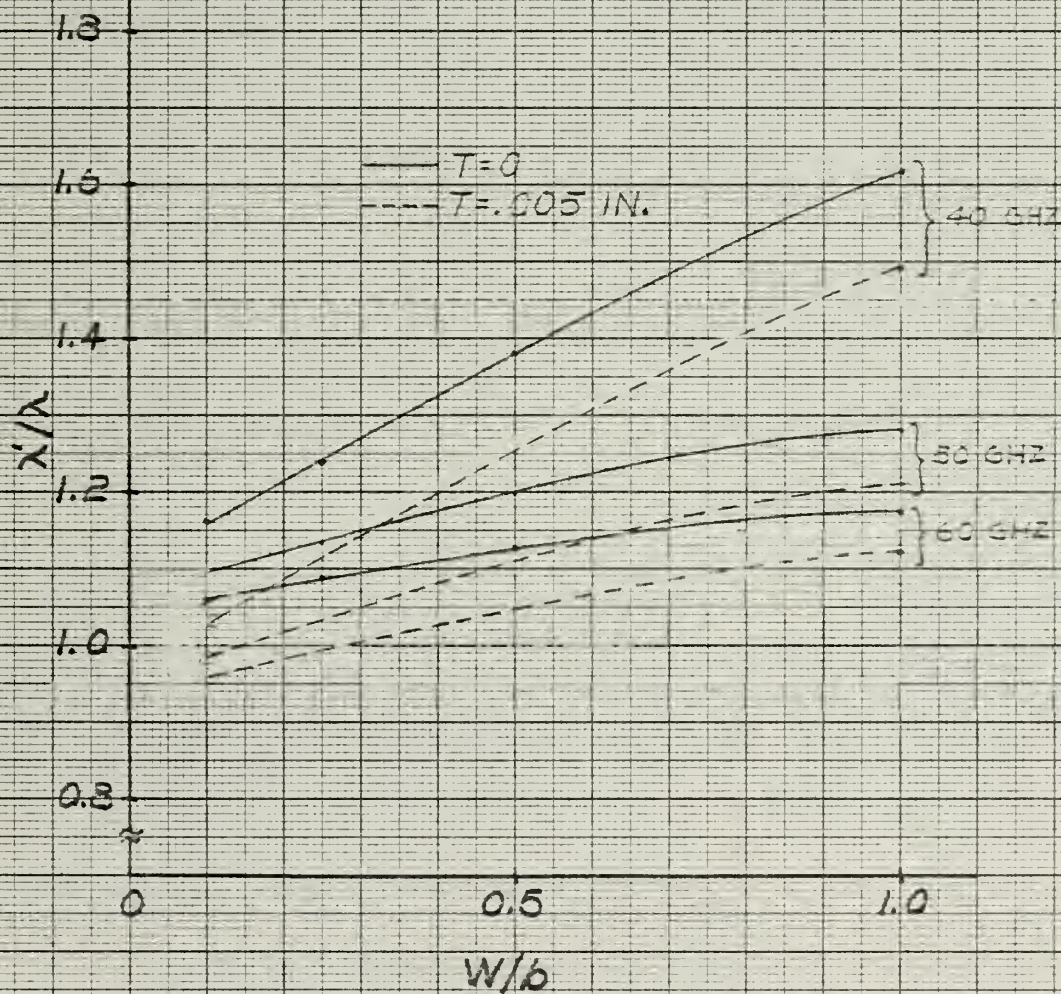
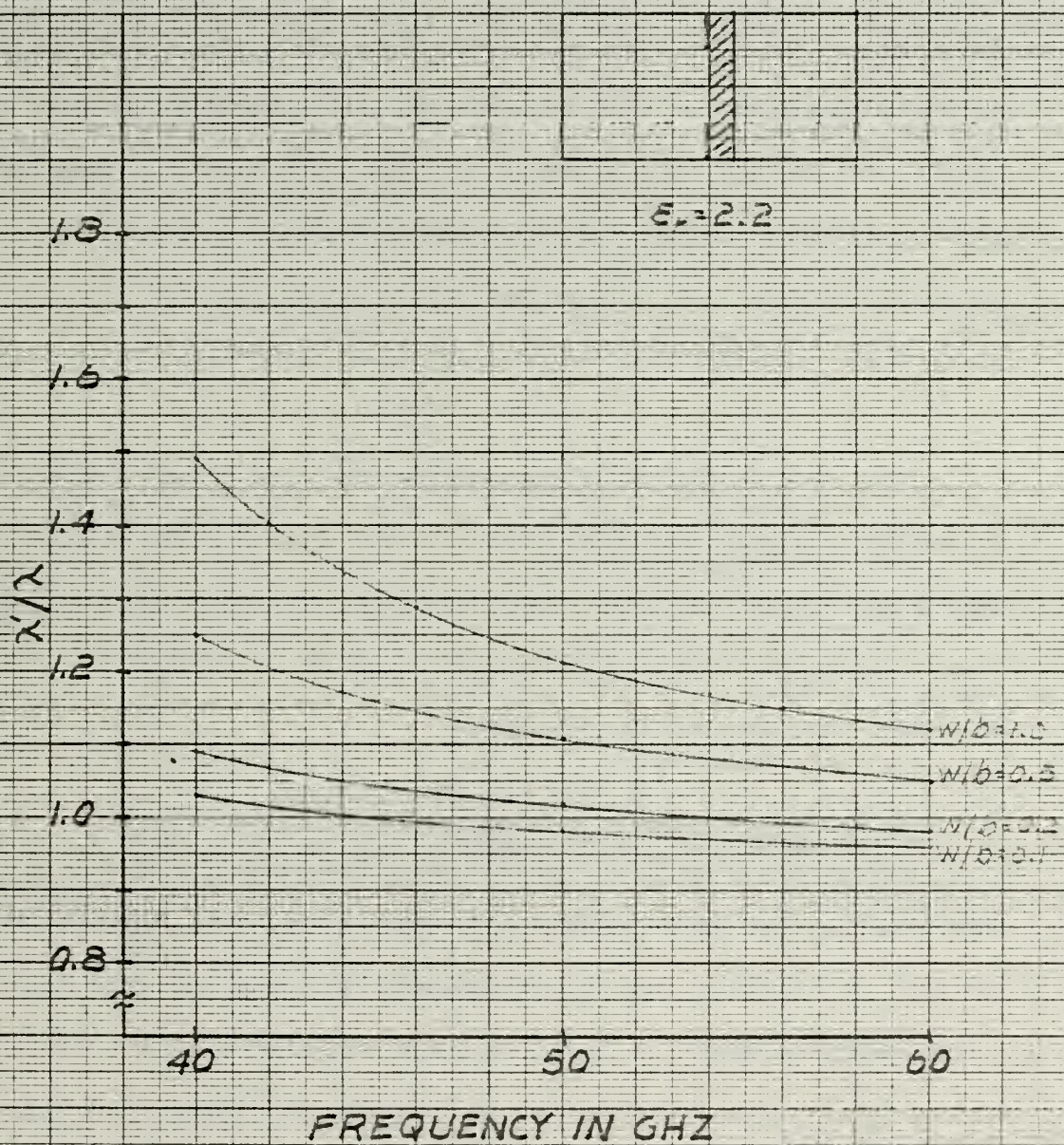




Figure 18 Normalized wavelength λ'/λ vs frequency
for U band fin line with $D = .005$ inches.



any intuitive or approximate methods valid for the entire range $0 < W/b \leq 1$. Several approaches were tried in this study and while results were "in the ball park" they were not deemed sufficiently accurate to present here.

The characteristic impedance for the case of small slot widths ($W/D < 2$) will eventually be obtained using Kuchler's program. As mentioned earlier this program is presently being rewritten to eliminate the overflow problems which prevented its application to the structures of interest in this study. Recall that Figure 9 showed the type of output available using this approach. That figure shows that the effect of the shield is to increase the characteristic impedance to a value greater than that for the corresponding open boundary structure.

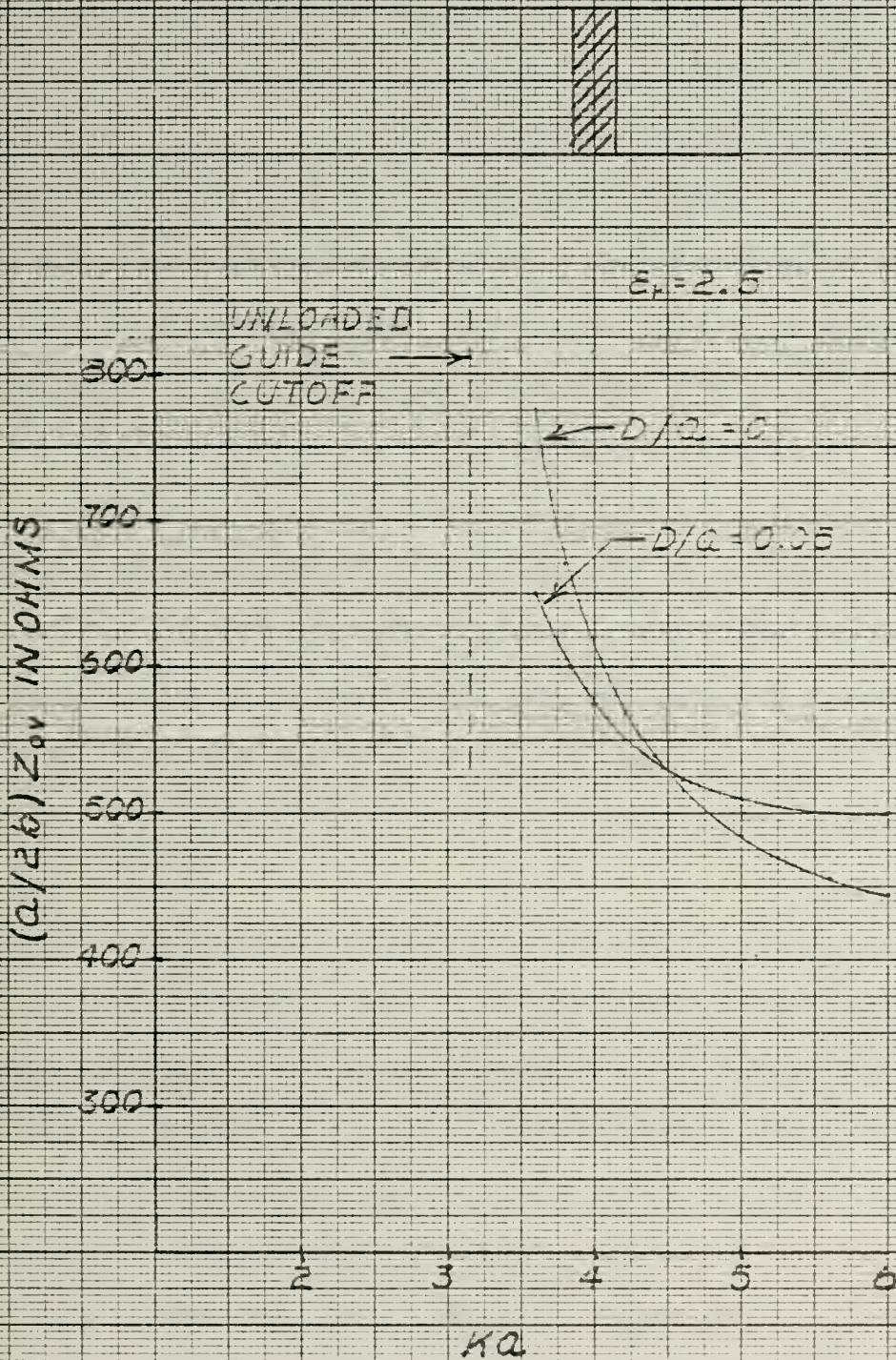
The characteristic impedance for the case $W/b = 1$ may be found exactly using a straightforward analytical approach. The functional form of the fields is known in each region and the wavelength ratio λ'/λ may be found as indicated in Appendix A. One can therefore evaluate

$$Z_{OV} = \frac{- \int E_y(a/2, Y) dy}{\iint \vec{E} \times \vec{H}^* \cdot \vec{A} z da} . \quad (9)$$

The utility of this result by itself was not deemed worth the effort of finding it, particularly in view of the fact that the calculation for $\epsilon_r = 2.5$ has been carried out by Vartanian [6]. His results are reproduced in Figure 19. The slab is centered in the waveguide and the impedance is defined as

$$Z_{OV} = \frac{V_O(a/2)}{2 P_{AVG}} . \quad (10)$$

Figure 19 Impedance vs normalized frequency $2\pi a/\lambda$
for a slab loaded rectangular waveguide.
 $\epsilon_r = 2.2$, slab centered (from ref. [6]).

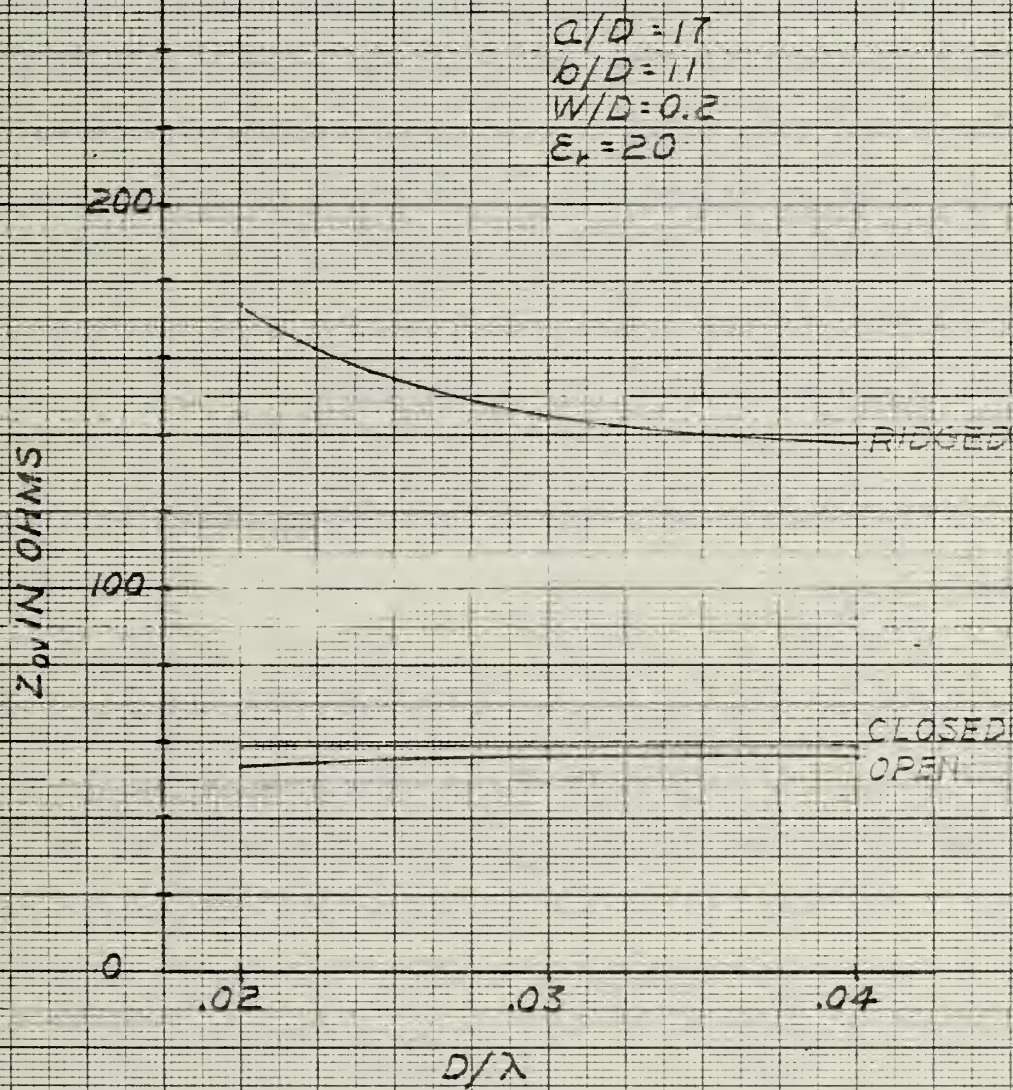


The slab location thickness and dielectric constant differ only slightly from the values of interest in this study. The results should therefore be qualitatively the same in all respects. The interesting feature revealed by Figure 19 is that the dielectric slab may cause either an increase or decrease in impedance depending upon frequency. At lower frequencies ($ka < 4.5$) the modification of cutoff wavelength appears to be the dominant effect while at higher frequencies ($ka > 4.5$) the increase in impedance is probably due to the concentration of a relatively higher field at guide center when the dielectric is present. In any event, the rather unpredictable nature of the characteristic impedance is clearly revealed.

The impedance of the structure of Figure 1 is probably of most interest when W/b is small. For this would be the geometry used to mount devices and the impedance is probably most relevant when considering device circuit interactions. Some observations may be made in this case.

Consider the structure examined by Kuchler and described earlier in relation to Figure 9. The characteristic impedance for the open and closed boundary structures has been reproduced in Figure 20 for the case $W/D = 0.2$. Also shown in Figure 20 is the impedance of the corresponding ridged waveguide structure ($b/a = .65$, $W/b = .018$). Clearly, if we view the composite structure as a dielectric loaded ridged waveguide then the effect of the dielectric is to lower the impedance. The apparent dielectric constant in this case is about 6; less than the

Figure 20 Characteristic impedance Z_{0v} vs frequency for open boundary slotline, shielded slotline and ridged waveguide.

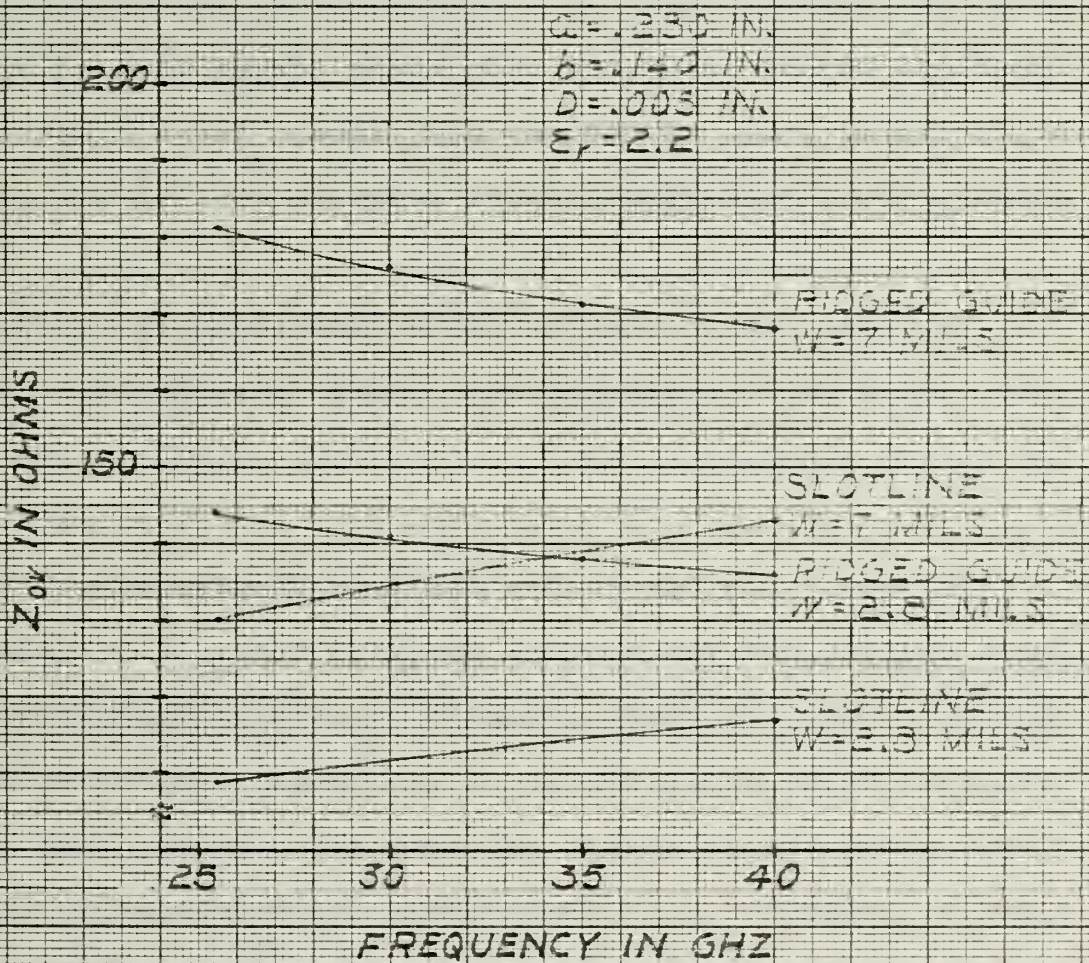


effective dielectric constant for wavelength ($\sim 8.2 - 9.5$) and certainly much less than the actual dielectric constant of $\epsilon_r = 20$. On the other hand, if we view the structure as a shielded slotline, then the effect of the shield is to increase the characteristic impedance of the unshielded slotline. In this particular situation, the field is tightly bound to the slot and there is not much interaction between the slot field and the shield. The composite structure behaves more like a slotline than a ridged waveguide. An important observation, however, is that the characteristic impedance of the composite structure is bounded from above by the ridged waveguide impedance and from below by the open boundary slotline impedance both of which are known for a wide range of parameters. In this particular case, the lower bound is tight and the upper bound is not. If the dielectric constant were decreased the impedance would approach the upper bound.

If the concept of bounding the impedance is applied to the K_a band structure of interest in this study, then we obtain the results illustrated in Figure 21. We see, for example, that for a 2.8 mil slot, the impedance at 30 GHz lies between 112 ohms and 140 ohms. If we estimate the impedance to be the average of these two values or 126 ohms the error would be only $\pm 12\%$ maximum. In fact, if we use the effective dielectric constant $k_e \sim 1.31$ which was determined earlier for use in calculating wavelength we would arrive at the following estimate of Z_{ov} for fin line:

$$Z_{ov} = \frac{Z_{ov}(\text{ridged})}{\sqrt{k_e}} = \frac{140}{\sqrt{1.31}} = 122 \text{ ohms}$$

Figure 21 Characteristic impedance vs frequency
for slotline and ridged waveguide in
 K_a band.



This is very close to the average of the two bounds. The expectation is however, that because of the low dielectric constant ($\epsilon_r = 2.2$) that the true impedance would be close to the ridged waveguide impedance.

The foregoing discussion suggests that the true impedance of fin line is probably very close to the impedance of the ridged waveguide substructure for the case where W/b is small and ϵ_r is not too large. Thus ridged waveguide impedance curves for K_a band and U band have been plotted in Figures 22 and 23 respectively using equation (4) and the parameters given in table 3. For $W/b < .1$ we believe that the fin line impedance may be estimated from these curves with an error of 10-15% maximum. Certainly they should serve a useful purpose until such time as more accurate results are available.

One last factor that should be mentioned is the fact that finite metal thickness will cause some decrease in impedance for narrow slots.

In summary, although the fin line impedance has not been found exactly for the general case $0 < W/b \leq 1$, it seems clear that for $W/b \lesssim .1$, $W/D \lesssim 2$ and ϵ_r small the impedance can be estimated quite accurately. It is bounded from above by the ridged waveguide impedance and from below by the open boundary slotline impedance. It is probably somewhat greater than

$$Z_{ov} = \frac{Z_{ov}(\text{ridged})}{\sqrt{k_e}} \quad (11)$$

where k_e is the effective dielectric constant from Figure 10. This places the impedance within about 10% of the ridged waveguide impedance given in Figures 22 and 23. The impedance is high even for small separation of fins; approximately 100-200 ohms.

Table 3. Parameters for calculation of K_a band and U band ridged waveguide impedance ($b/a = .5$).

| W/b | $Z_{ov\infty}$ (ohms) | λ_c/a | $K_a \lambda_c$ (cm) | $U \lambda_c$ (cm) |
|-------|--------------------------|---------------|----------------------|--------------------|
| .02 | 130 | 3.66 | 2.60 | 1.75 |
| .05 | 160 | 3.38 | 2.40 | 1.61 |
| .10 | 190 | 3.08 | 2.19 | 1.47 |
| .25 | 256 | 2.66 | 1.89 | 1.27 |
| .50 | 317 | 2.28 | 1.62 | 1.09 |
| 1.0 | 377 | | 1.42 | 0.96 |

5.0 Conclusions

The center finned, dielectric loaded rectangular waveguide (fin line) may be viewed variously as a shielded slotline, a dielectric loaded ridged waveguide or a slab loaded rectangular waveguide ($W/b = 1$). Each of these substructures has been studied to some extent and therefore it is possible by combining results for the different substructures to piece together the desired solution. This has been successfully accomplished for the wavelength ratio λ'/λ vs frequency with W/b as a parameter. The accuracy of this solution is estimated to be no worse than 5% for small values of W/b and as good as $\frac{1}{2}\%$ for $W/b = 1$.

46

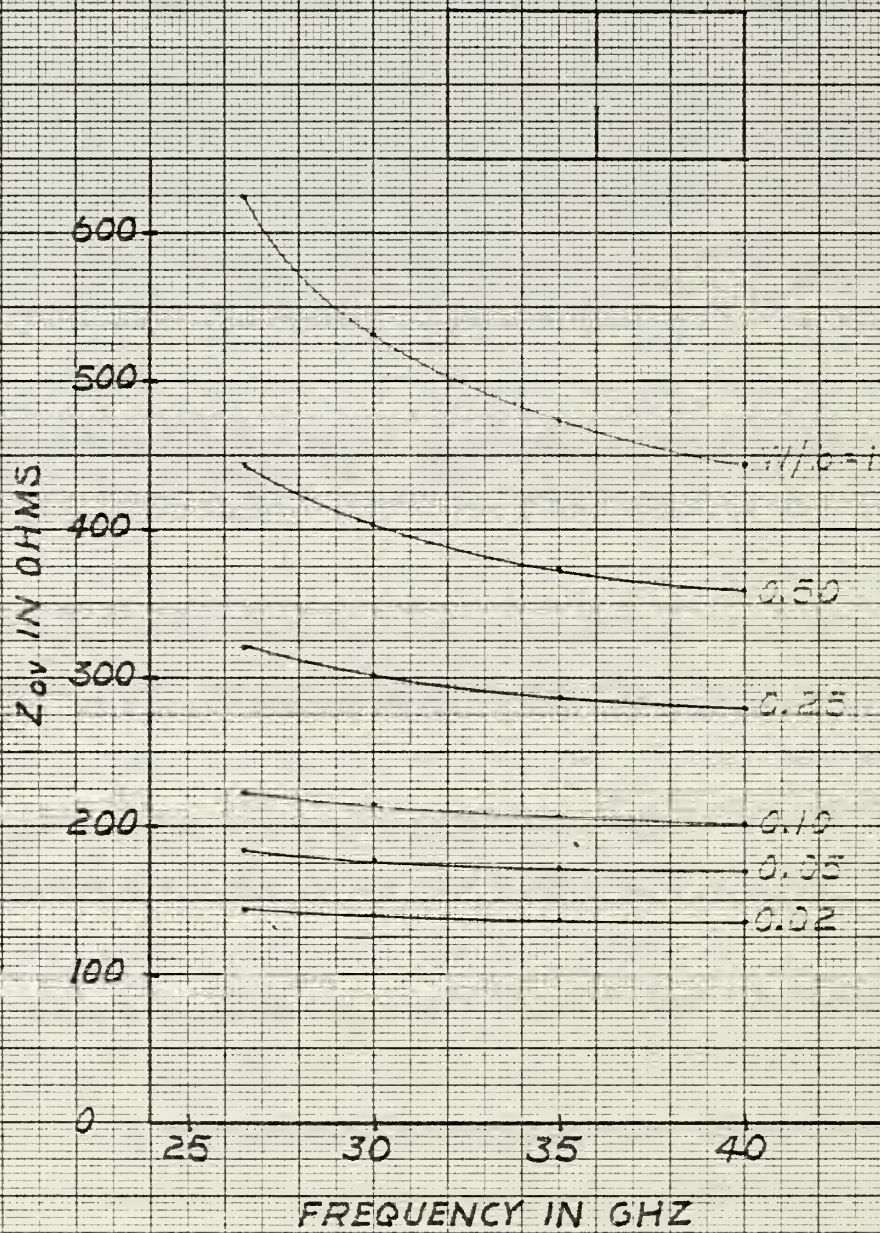
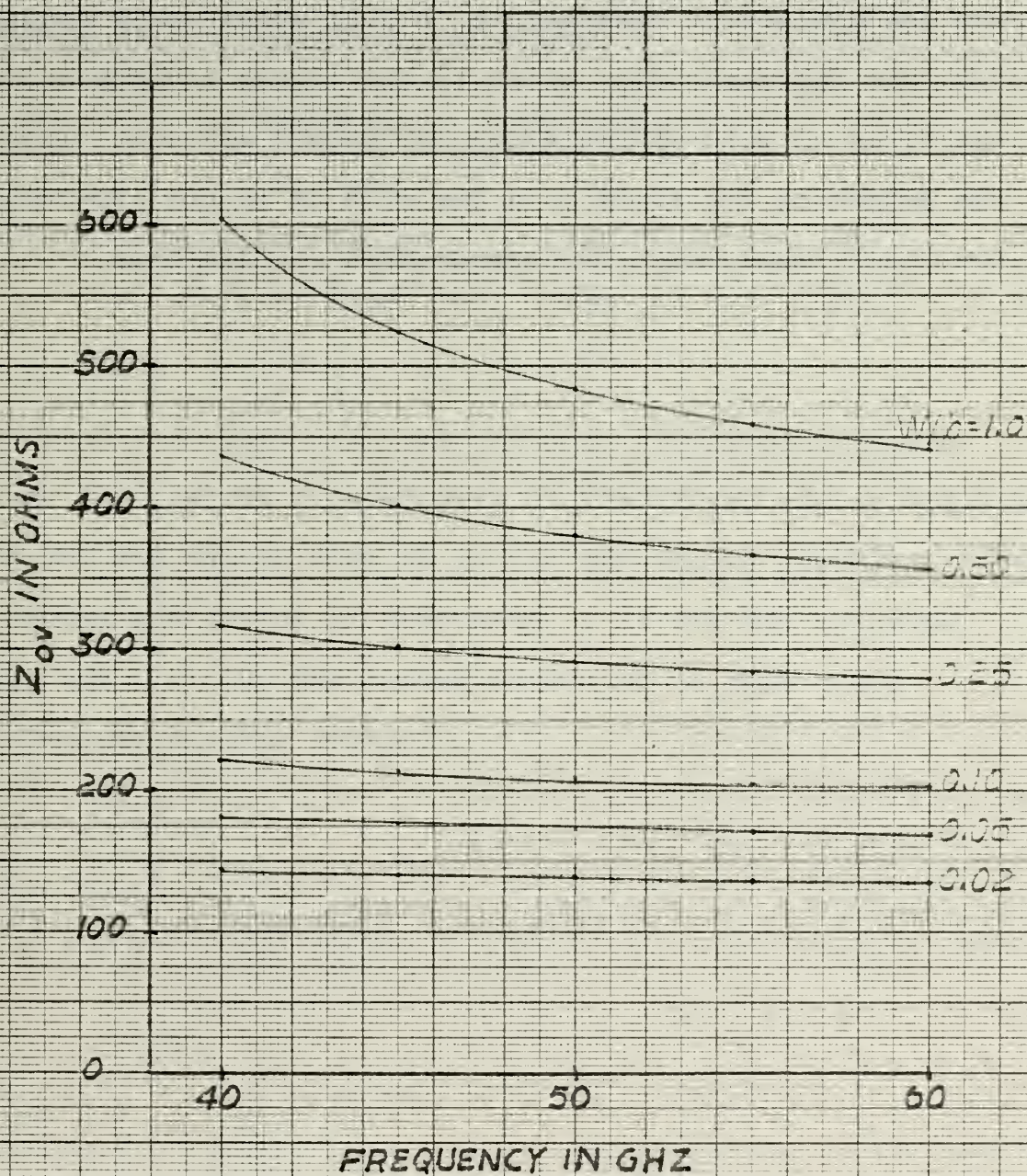


Figure 23 Characteristic impedance vs frequency for U band ridged waveguide.



The characteristic impedance is more difficult to establish and for the general case $0 < W/b \leq 1$ was not determined in this study. However, for small fin separation the characteristic impedance has been bounded from above and below by the ridged waveguide impedance and the open boundary slotline impedance. The tightness of the bounds is such that taking the mean as an estimate would result in an error of only $\pm 10-15\%$. Taking into account the low dielectric constant ($\epsilon_r = 2.2$) which would suggest that the true impedance lies close to the ridged waveguide impedance the error in this estimate can be further reduced. In any event, the impedance for slots of a few mils is in the 100-200 ohm range for the K_a band and U band structures studied here.

Appendix A. Slab Loaded Rectangular Waveguide Program

The slab loaded rectangular waveguide problem addressed in section 2.3 of this report was solved using a program written to run on a Wang 500 or Wang 600 Programmable Calculator with drum printer. The program solves equation (5) by an iterative search for the correct value of λ'/λ . The following data is required to be entered in the registers indicated:

| Input Data | Register |
|--------------|----------|
| d_1 (cm) | 00 |
| d_2 (cm) | 01 |
| t (cm) | 02 |
| ϵ_r | 11 |

After entering this data into the machine, the program is run by entering the desired frequency in gigahertz and keying "SEARCH", "1". The DEG/RAD switch must be in the RAD (down) position. The program causes a printout of frequency, λ'/λ for the unloaded waveguide, and λ'/λ for the loaded waveguide in that order.

The program listing follows.

| | | | | | | | |
|-----|----|----|-----------------|-----|----|----|-----------------|
| 000 | 09 | 00 | * M | 080 | 07 | 06 | RE 6 |
| 001 | 00 | 01 | E 1 | 081 | 06 | 14 | ST 14 |
| 002 | 08 | 02 | * W | 082 | 07 | 01 | RE 1 |
| 003 | 06 | 02 | ST 2 | 083 | 04 | 14 | × 14 |
| 004 | 08 | 15 | * $\frac{1}{2}$ | 084 | 08 | 08 | * IN |
| 005 | 06 | 03 | ST 3 | 085 | 08 | 15 | * $\frac{1}{2}$ |
| 006 | 00 | 03 | E 3 | 086 | 06 | 14 | ST 14 |
| 007 | 00 | 00 | E 0 | 087 | 07 | 06 | RE 6 |
| 008 | 04 | 03 | × 3 | 088 | 04 | 14 | × 14 |
| 009 | 06 | 14 | ST 14 | 089 | 00 | 12 | E 12 |
| 010 | 07 | 00 | RE 0 | 090 | 06 | 09 | ST 9 |
| 011 | 06 | 15 | ST 15 | 091 | 06 | 10 | ST 10 |
| 012 | 07 | 01 | RE 1 | 092 | 07 | 06 | RE 6 |
| 013 | 02 | 15 | + 15 | 093 | 06 | 14 | ST 14 |
| 014 | 07 | 02 | RE 2 | 094 | 07 | 00 | RE 0 |
| 015 | 02 | 15 | + 15 | 095 | 04 | 14 | × 14 |
| 016 | 00 | 02 | E 2 | 096 | 06 | 06 | * IN |
| 017 | 04 | 15 | × 15 | 097 | 06 | 14 | ST 14 |
| 018 | 05 | 14 | ÷ 14 | 098 | 07 | 05 | RE 5 |
| 019 | 08 | 12 | * x^2 | 099 | 04 | 14 | × 14 |
| 020 | 00 | 12 | E 12 | 100 | 07 | 06 | RE 6 |
| 021 | 06 | 14 | ST 14 | 101 | 05 | 14 | ÷ 14 |
| 022 | 00 | 01 | E 1 | 102 | 09 | 08 | * T |
| 023 | 02 | 14 | + 14 | 103 | 06 | 07 | ST 7 |
| 024 | 08 | 13 | * \sqrt{x} | 104 | 07 | 05 | RE 5 |
| 025 | 08 | 15 | * $\frac{1}{2}$ | 105 | 08 | 14 | ST 14 |
| 026 | 06 | 04 | ST 4 | 106 | 07 | 02 | RE 2 |
| 027 | 08 | 02 | * W | 107 | 04 | 14 | × 14 |
| 028 | 06 | 03 | ST 3 | 108 | 07 | 07 | RE 7 |
| 029 | 00 | 10 | E 10 | 109 | 02 | 14 | + 14 |
| 030 | 00 | 00 | E 0 | 110 | 08 | 08 | * IN |
| 031 | 00 | 00 | E 0 | 111 | 08 | 15 | * $\frac{1}{2}$ |
| 032 | 00 | 05 | E 5 | 112 | 06 | 14 | ST 14 |
| 033 | 03 | 04 | - 4 | 113 | 07 | 05 | RE 5 |
| 034 | 09 | 00 | * M | 114 | 04 | 14 | × 14 |
| 035 | 00 | 02 | E 2 | 115 | 00 | 12 | E 12 |
| 036 | 10 | 02 | f 2 | 116 | 06 | 08 | ST 8 |
| 037 | 08 | 05 | * J+ | 117 | 02 | 10 | + 10 |
| 038 | 10 | 03 | f 3 | 118 | 09 | 15 | * RT |
| 039 | 06 | 03 | * Go | 119 | 09 | 00 | * M |

| | | | | | | | |
|-----|----|----|-----------------|-----|----|----|-------|
| 040 | 00 | 10 | E10 | 120 | 10 | 03 | f 3 |
| 041 | 00 | 00 | E0 | 121 | 07 | 04 | RE 4 |
| 042 | 00 | 00 | E0 | 122 | 06 | 02 | * W |
| 043 | 00 | 05 | E5 | 123 | 07 | 03 | RE 3 |
| 044 | 03 | 04 | - 4 | 124 | 08 | 02 | * W |
| 045 | 08 | 00 | * S | 125 | 07 | 15 | RE 15 |
| 046 | 00 | 02 | E 2 | 126 | 09 | 03 | * SP |
| 047 | 09 | 00 | * M | 127 | 09 | 14 | * EP |
| 048 | 10 | 02 | f 2 | | | | |
| 049 | 09 | 02 | * α | | | | |
| 050 | 10 | 00 | f 0 | | | | |
| 051 | 06 | 15 | ST15 | | | | |
| 052 | 00 | 02 | E 2 | | | | |
| 053 | 04 | 15 | $\times 15$ | | | | |
| 054 | 07 | 03 | RE 3 | | | | |
| 055 | 05 | 15 | $\div 15$ | | | | |
| 056 | 06 | 12 | * x^2 | | | | |
| 057 | 06 | 15 | ST15 | | | | |
| 058 | 07 | 04 | RE 4 | | | | |
| 059 | 08 | 15 | * $\frac{1}{2}$ | | | | |
| 060 | 08 | 12 | * x^2 | | | | |
| 061 | 00 | 12 | E12 | | | | |
| 062 | 06 | 14 | ST14 | | | | |
| 063 | 00 | 01 | E 1 | | | | |
| 064 | 02 | 14 | +14 | | | | |
| 065 | 07 | 15 | RE15 | | | | |
| 066 | 04 | 14 | $\times 14$ | | | | |
| 067 | 08 | 13 | * \sqrt{x} | | | | |
| 068 | 06 | 06 | ST 6 | | | | |
| 069 | 07 | 04 | RE 4 | | | | |
| 070 | 08 | 15 | * $\frac{1}{2}$ | | | | |
| 071 | 08 | 12 | * x^2 | | | | |
| 072 | 00 | 12 | E12 | | | | |
| 073 | 06 | 14 | ST14 | | | | |
| 074 | 07 | 11 | RE11 | | | | |
| 075 | 02 | 14 | +14 | | | | |
| 076 | 07 | 15 | RE15 | | | | |
| 077 | 04 | 14 | $\times 14$ | | | | |
| 078 | 08 | 13 | * \sqrt{x} | | | | |
| 079 | 06 | 05 | ST 5 | | | | |

List of References

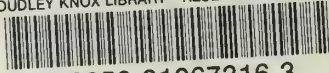
1. P. J. Meier, "Integrated Fin-Line Millimeter Components," IEEE Trans. Microwave Theory and Tech., vol.MTT-22, pp.1209-1216, December 1974.
2. S. B. Cohn, "Slotline on a Dielectric Substrate," IEEE Trans. Microwave Theory and Tech., vol.MTT-17, pp. 768-778, October 1969.
3. J. B. Knorr and K-D. Kuchler, "Analysis of Coupled Slots and Coplanar Strips on a Dielectric Substrate," IEEE Trans. Microwave Theory and Tech., vol. MTT-23, pp.541-548, July 1975.
4. S. Hopfer, "The Design of Ridged Waveguides," IRE Trans.- Microwave Theory and Techniques, vol. MTT-3, pp. 20-29, October 1955.
5. R. O. Lagerlöf, "Ridged Waveguide for Planar Microwave Circuits," IEEE Trans. Microwave Theory and Techniques, vol. MTT-21, pp.499-501, July 1973.
6. P. H. Vartanian, et al., "Propagation in Dielectric Slab Loaded Rectangular Waveguide," IRF Trans. Microwave Theory and Tech., vol. MTT-6, pp.215-222, April 1958.
7. R. Collin, Field Theory of Guided Waves. New York: McGraw Hill, 1960.
8. K. D. Kuchler, "Hybrid Mode Analysis of Coplanar Transmission Lines," Ph.D. Thesis, Naval Postgraduate School, June 1975.
9. J. B. Knorr and A. Tufekcioglu, "Spectral Domain Calculation of Microstrip Characteristic Impedance," IEEE Trans. Microwave Theory and Tech., vol. MTT-23, pp. 725-728, September 1975.

Distribution List

| | |
|---|----|
| Defense Documentation Center Cameron Station Alexandria, Virginia 22314 | 12 |
| Library Naval Postgraduate School Monterey, California 93940 | 2 |
| Office of Research Administration Naval Postgraduate School Monterey, California 93940 | 1 |
| Chairman, Department of Electrical Engineering Naval Postgraduate School Monterey, California 93940 | 1 |
| Professor Jeffrey B. Knorr Department of Electrical Engineering Naval Postgraduate School Monterey, California 93940 | 10 |
| Dr. Tom Kihm Microwave Technology Branch - Code 2330 Naval Electronics Laboratory Center San Diego, California | 2 |

U177739

DUDLEY KNOX LIBRARY - RESEARCH REPORTS



5 6853 01067316 3

~~U17773~~

M